expression levels were about 2.5 times higher in colon tissue obtained from BALB/c mice with DSS-induced colitis and treated with HNP-1 compared with those that did not receive HNP-1 (data not shown), although the cell types in which IL-1β was expressed were not clear; candidate populations include lamina propria CD11b macrophages and intestinal epithelial cells. HNP-1 also affected IL-1β expression in SCID mice with DSS-induced colitis, although TNF-α and IFN-γ were not detected in ex vivo experiments. Furthermore, the cells recruited to the inflamed colonic mucosa in mice with DSS-induced colitis were mainly macrophages, which increased in number following HNP-1 treatment of BALB/c mice. Similar results were observed in SCID mice, which lack lymphocytes. HNP-1–3 increase inflammatory cell migration[12,19] and cause macrophages to secrete TNF-α and IFN-γ.[20] HNP-1 reportedly upregulated expression levels of TNF-α and IL-1β in monocytes activated by *Staphylococcus aureus* or phorbol myristate acetate (PMA).[21] A porcine neutrophil antimicrobial peptide similar to defensins and HNP-1 has been shown to modify IL-1 release.[34] In addition, Granz et al[35] reported that direct cellular contact with stimulated T cells induces the expression/activation of proinflammatory factors and pathways in human monocytes. Thus, HNP-1 may primarily affect IL-1β secretion by macrophages in SCID mice and expression of TNF-α and IFN-γ may require T-cell binding in BALB/c mice; this effect may require stimulatory conditions, such as DSS-induced colitis.

Our in vitro studies indicate that HNP-1 has both inhibitory and promoting effects on colon epithelial cell proliferation, although it should be noted that we used cancer cells (Fig. 6). HNP-1 at low concentrations was shown to enhance cell proliferation, whereas high HNP-1 concentrations reduced the proliferation of respiratory epithelial cells, blood corpuscle origin cells, and oral squamous carcinoma cells.[22–25] In contrast, the effects of HNP-1 on Ki-67 immunostaining in colon epithelial cells from mice with DSS-induced colitis were similar among BALB/c and SCID mice treated with HNP-1 or PBS (Figs. 3D, 6D). Although HNP-1 levels may not reach 100 μg/mL under normal physiologic conditions (Fig. 7A), HNP-1–3 levels in patients with bacterial infections can certainly exceed this concentration.[36] Furthermore, local concentrations of HNP-1–3 at the site of inflammation are likely higher than plasma levels.[33] Although in vitro assays may not reveal all of the in vivo effects of HNP-1, we have described a possible mechanism by which HNP-1–3 aggravate UC. Furthermore, although the effects of HNP-1 on cell proliferation are likely not specific to colon epithelial cells,[33] the cytotoxicity of HNP-1 in colon epithelial cells, together with dysregulated inflammatory cytokine expression, may contribute to colitis.[37] Further examinations are needed to build on our results—for example, in vitro assays using normal colon epithelial cells with relatively low concentrations of HNP-1 and assays of regional HNP-1–3 concentrations in patients with UC.

HNP-1–3 are antimicrobial and help to prevent bacterial infections that can contribute to IBD.[38] Moreover, neutrophils were recently shown to be an important source of the potent immunosuppressive cytokine IL-10 at the site of infection during sepsis.[39] On the other hand, leukocytapheresis is an effective method to treat UC. TNF-α and IL-1β levels are reduced by leukocytapheresis,[3,4] and removing activated leukocytes may reduce HNP-1–3 levels, resulting in lower inflammatory cytokine concentrations and reduced colonic inflammation. Thus, although HNP-1–3 may produce both beneficial and pathologic effects, patients with UC are likely to benefit from reducing high expression levels of HNP-1–3.

In conclusion, HNP-1 may aggravate UC, in part, by elevating levels of inflammatory cytokines, including TNF-α, IFN-γ, and IL-1β, potentially via a T-cell-independent pathway.

ACKNOWLEDGMENT

We thank Ms. Yuko Morinaga for technical assistance.

REFERENCES

1. Podolsky DK. Inflammatory bowel disease. N Engl J Med. 2002;347:417–429.
2. Murch SH, Lamkin VA, Savage MO, et al. Serum concentrations of tumour necrosis factor alpha in childhood chronic inflammatory bowel disease. Gut. 1991;32:913–917.
3. Sawada K, Ohnishi K, Kosaka T, et al. Leukocytapheresis with leukocyte removal filter as new therapy for ulcerative colitis. Ther Apher. 1997;1:207–211.
4. Yamamoto T, Saniabadi AR, Umegae S, et al. Impact of selective leukocytapheresis on mucosal inflammation and ulcerative colitis: cytokine profiles and endoscopic findings. Inflamm Bowel Dis. 2006;12:719–726.
5. Ganz T. Defensins: antimicrobial peptides of vertebrates. C R Biol. 2004;327:539–549.
6. Ganz T, Lehrer RI. Defensins. Curr Opin Immunol. 1994;6:584–589.
7. Lichtenstein AK, Ganz T, Nguyen TM. Mechanism of target cytolysis by peptide defensins. Target cell metabolic activities, possibly involving endocytosis, are crucial for expression of cytotoxicity. J Immunol. 1988;140:2686–2694.
8. Van Wetering S, Mannesse-Lazeroms SP, Dijkman JH, et al. Effect of neutrophil serine proteinases and defensins on lung epithelial cells: modulation of cytotoxicity and IL-8 production. J Leukoc Biol. 1997;62:217–226.
9. Ganz T, Selsted ME, Szklarek D, et al. Defensins. Natural peptide antibiotics of human neutrophils. J Clin Invest. 1985;76:1427–1435.
10. Kanmura S, Uto H, Numata M, et al. Human neutrophil peptides 1–3 are useful biomarkers in patients with active ulcerative colitis. Inflamm Bowel Dis. 2009;15:909–917.
11. Liu CT, Lin HC, Yu CT, et al. The concentration-dependent chemokine release and pro-apoptotic effects of neutrophil-derived α-defensin-1 on human bronchial and alveolar epithelial cells. Life Sci. 2007;80:749–758.
12. Jasmin G, Afsaneh S, Ulf F, et al. Chemoattraction of macrophages, T lymphocytes, and mast cells is evolutionarily conserved within the human α-defensin family. J Immunol. 2007;179:3958–3965.
13. Murthy SN, Cooper HS, Shim H, et al. Treatment of dextran sulfate sodium-induced murine colitis by intracolonic cyclosporin. Dig Dis Sci. 1993;38:1722–1734.

14. Cooper HS, Murthy SN, Shah RS, et al. Clinicopathologic study of dextran sulfate sodium experimental murine colitis. Lab Invest. 1993; 69:238–249.
15. Qualls JE, Tuna H, Kaplan AM, et al. Suppression of experimental colitis in mice by CD11c+ dendritic cells. Inflamm Bowel Dis. 2009; 15:236–247.
16. Khan WI, Motomura Y, Wang H, et al. Critical role of MCP-1 in the pathogenesis of experimental colitis in the context of immune and enterochromaffin cells. Am J Physiol Gastrointest Liver Physiol. 2006; 291:G803–G811.
17. Ohda Y, Hori K, Tomita T, et al. Effects of hepatocyte growth factor on rat inflammatory bowel disease models. Dig Dis Sci. 2005;50: 914–921.
18. Azuma YT, Hagi K, Shintani N, et al. PACAP provides colonic protection against dextran sodium sulfate induced colitis. J Cell Physiol. 2008;216:111–119.
19. Chertov O, Michiel DF, Xu L, et al. Identification of defensin-1, defensin-2, and CAP37/azurocidin as T-cell chemoattractant proteins released from interleukin-8-stimulated neutrophils. J Biol Chem. 1996; 271:2935–2940.
20. Soehnlein O, Kai-Larsen Y, Frithiof R, et al. Neutrophil primary granule proteins HBP and HNP1–3 boost bacterial phagocytosis by human and murine macrophages. J Clin Invest. 2008;118:3491–3502.
21. Chaly YV, Paleolog EM, Kolesnikova TS, et al. Neutrophil alpha-defensin human neutrophil peptide modulates cytokine production in human monocytes and adhesion molecule expression in endothelial cells. Eur Cytokine Netw. 2000;11:257–266.
22. Aarbiou J, Ertmann M, van Wetering S, et al. Human neutrophil defensins induce lung epithelial cell proliferation in vitro. J Leukoc Biol. 2002;72:167–174.
23. Lichtenstein AK, Ganz T, Selsted ME, et al. In vitro tumor cell cytolysis mediated by peptide defensins of human and rabbit granulocytes. Blood. 1986;68:1407–1410.
24. Sakamoto N, Mukae H, Fujii T, et al. Differential effects of alpha- and beta-defensin on cytokine production by cultured human bronchial epithelial cells. Am J Physiol Lung Cell Mol Physiol. 2005;288:508–513.
25. McKeown ST, Lundy FT, Nelson J, et al. The cytotoxic effects of human neutrophil peptide-1 (HNP1) and lactoferrin on oral squamous cell carcinoma (OSCC) in vitro. Oral Oncol. 2006;42:685–690.
26. Swidsinski A, Ladhoff A, Pernthaler A, et al. Mucosal flora in inflammatory bowel disease. Gastroenterology. 2002;22:44–54.
27. Ohkusa T, Okayasu I, Tokoi S, et al. Bacterial invasion into the colonic mucosa in ulcerative colitis. J Gastroenterol Hepatol. 1993;8: 116–118.
28. Lampinen M, Rönnblom A, Amin K, et al. Eosinophil granulocytes are activated during the remission phase of ulcerative colitis. Gut. 2005;54:1714–1720.
29. Tollin M, Bergman P, Svenberg T, et al. Antimicrobial peptides in the first line defence of human colon mucosa. Peptides. 2003;24:523–530.
30. Cunliffe RN, Kamal M, Rose FR, et al. Expression of antimicrobial neutrophil defensins in epithelial cells of active inflammatory bowel disease mucosa. J Clin Pathol. 2002;55:298–304.
31. Zou H, Harrington JJ, Sugumar A, et al. Detection of colorectal disease by stool defensin assay: an exploratory study. Clin Gastroenterol Hepatol. 2007;5:865–868.
32. Ashitani J, Mukae H, Hiratsuka T, et al. Elevated levels of alpha-defensins in plasma and BAL fluid of patients with active pulmonary tuberculosis. Chest. 2002;121:519–526.
33. Soong LB, Ganz T, Ellison A, et al. Purification and characterization of defensins from cystic fibrosis sputum. Inflamm Res. 1997;46:98–102.
34. Perregaux DG, Bhavsar K, Contillo L, et al. Antimicrobial peptides initiate IL-1 beta posttranslational processing: a novel role beyond innate immunity. J Immunol. 2002;168:3024–3032.
35. Gruaz L, Delucinge-Vivier C, Descombes P, et al. Blockade of T cell contact-activation of human monocytes by high-density lipoproteins reveals a new pattern of cytokine and inflammatory genes. PLoS One. 2010;5:e9418.
36. Panyutich AV, Panyutich EA, Krapivin VA, et al. Plasma defensin concentrations are elevated in patients with septicemia or bacterial meningitis. J Lab Clin Med. 1993;122:202–207.
37. Hansen R, Thomson JM, El-Omar EM, et al. The role of infection in the actiology of inflammatory bowel disease. J Gastroenterol. 2010;45: 266–276.
38. Mayer L. Evolving paradigms in the pathogenesis of IBD. J Gastroenterol. 2010;45:9–16.
39. Kasten KR, Muenzer JT, Caldwell CC. Neutrophils are significant producers of IL-10 during sepsis. Biochem Biophys Res Commun. 2010; 393:28–31.

ORIGINAL ARTICLE

Oncogenic Smad3 Signaling Induced by Chronic Inflammation Is an Early Event in Ulcerative Colitis-associated Carcinogenesis

Seiji Kawamata, MD, Koichi Matsuzaki, MD,* Miki Murata, MD,* Toshihito Seki, MD,* Katsuyoshi Matsuoka, MD,† Yasushi Iwao, MD,‡ Toshifumi Hibi, MD,† and Kazuichi Okazaki, MD**

Background: Both chronic inflammation and somatic mutations likely contribute to the pathogenesis of ulcerative colitis (UC)-associated dysplasia and cancer. On the other hand, both tumor suppression and oncogenesis can result from transforming growth factor (TGF)-β signaling. TGF-β type I receptor (TβRI) and Ras-associated kinases differentially phosphorylate a mediator, Smad3, to become C-terminally phosphorylated Smad3 (pSmad3C), linker phosphorylated Smad3 (pSmad3L), and both C-terminally and linker phosphorylated Smad3 (pSmad3L/C). The pSmad3C/$p21^{WAF1}$ pathway transmits a cytostatic TGF-β signal, while pSmad3L and pSmad3L/C promote cell proliferation by upregulating c-Myc oncoprotein. The purpose of this study was to clarify the alteration of Smad3 signaling during UC-associated carcinogenesis.

Methods: By immunostaining and immunofluorescence, we compared pSmad3C-, pSmad3L-, and pSmad3L/C-mediated signaling in colorectal specimens representing colitis, dysplasia, or cancer from eight UC patients with signaling in normal colonic crypts. We also investigated p53 expression and mutations of *p53* and *K-ras* genes. We further sought functional meaning of the phosphorylated Smad3-mediated signaling in vitro.

Results: As enterocytes in normal crypts migrated upward toward the lumen, cytostatic pSmad3C/$p21^{WAF1}$ tended to increase, while pSmad3L/c-Myc shown by progenitor cells gradually decreased. Colitis specimens showed prominence of pSmad3L/C/c-Myc, mediated by TGF-β and tumor necrosis factor (TNF)-α, in all enterocyte nuclei throughout entire crypts. In proportion with increases in frequency of *p53* and *K-ras* mutations during progression from dysplasia to cancer, the oncogenic pSmad3L/c-Myc pathway came to be dominant with suppression of the pSmad3C/$p21^{WAF1}$ pathway.

Conclusions: Oncogenic Smad3 signaling, altered by chronic inflammation and eventually somatic mutations, promotes UC-associated neoplastic progression by upregulating growth-related protein.

(Inflamm Bowel Dis 2011;17:683–695)

Key Words: TGF-β, Smad, c-Jun N-terminal kinase, TNF-α, biomarker

Patients with ulcerative colitis (UC) are at increased risk for developing colorectal cancer.[1] The prevalence of UC-associated colorectal cancer, now referred to as colitic cancer, has steadily increased world wide.[2] The consensus is established that colitic cancer is preceded by dysplasia.[3] The "adenoma-carcinoma" sequence found in sporadic colorectal cancer can be replaced by a "colitis-dysplasia-carcinoma" sequence in UC.[4]

To date, no known genetic basis has been identified to explain the colorectal cancer predisposition in UC.[5] One therefore suspects that chronic inflammation as the cause of cancer: a hypothesis supported by clinical evidence that colorectal cancer risk increases with a longer duration of UC and anatomic extent of UC.[6] Additionally, certain drugs used to treat inflammation may prevent the development of colorectal cancer.[7] The major oncogenic pathways that lead to sporadic colorectal cancer, namely, chromosomal instability, microsatellite instability, and hypermethylation, also occur in colitic cancer.[8–10]

Transforming growth factor (TGF)-β can inhibit intestinal epithelial cell growth, acting as a tumor suppressor. During carcinogenesis, however, cancer cells gain an advantage by selective reduction of the tumor-suppressive activity of TGF-β together with augmentation of its oncogenic activity.[11] We therefore hypothesized that alteration of TGF-β signaling could lead to development of cancer in long-standing UC.

Smads are central mediators of signals transduced from the receptors for TGF-β superfamily members to the cell nucleus.[12] Smads are modular proteins with conserved

Received for publication March 26, 2010; Accepted May 19, 2010.

From the *Department of Gastroenterology and Hepatology, Kansai Medical University, Osaka, Japan; and †Division of Gastroenterology and Hepatology, Department of Internal Medicine, Keio University School of Medicine, Tokyo, Japan, ‡Center for Diagnostic and Therapeutic Endoscopy, Keio University School of Medicine, Tokyo, Japan.

Supported by the Ministry of Education, Science and Culture of Japan to K.M. (C16590646); and by Health and Labor Science Research Grants from the Japanese Ministry of Health, Labor and Welfare, and Research on Measures for Intractable Disease (Inflammatory Bowel Disease) to K.O.

Reprints: Koichi Matsuzaki, MD, Departments of Gastroenterology and Hepatology, Kansai Medical University, 10-15 Fumizonocho, Moriguchi, Osaka, 570-8506, Japan (e-mail: matsuzak@takii.kmu.ac.jp)

DOI 10.1002/ibd.21395

Published online 2 July 2010 in Wiley Online Library (wileyonlinelibrary.com).

TABLE 1. Clinicopathologic Features and Smad3 Phosphorylation in Colon Specimens from Patients with Colitic Cancer

Patient	Age	Sex	Duration (years)	UC Location	Cancer Histology[b]	pSmad3L SI (%)[a]			pSmad3C SI (%)[a]		
						Colitis	Dysplasia	Cancer	Colitis	Dysplasia	Cancer
1	28	M	10	Total	Well	18	33	46	85	82	71
2	42	F	15	Total	Well	43	58	63	78	76	69
3	48	M	12	Total	Well	32	34	36	74	73	70
4	40	M	18	Left	Well	33	37	48	81	75	67
5	30	M	9	Left	Well	78	85	87	94	79	73
6	60	M	22	Left	Moderate	14	76	81	78	71	66
7	43	M	22	Total	Well	65	92	96	91	88	57
8	29	F	19	Total	Well	67	87	94	98	83	81

pSmad3L, linker-phosphorylated Smad3; pSmad3C, C-terminally phosphorylated Smad3.
[a]Immunostained index (SI) represents the average percentage of immunoreactive cells.
[b]Histological grading of colitic cancer is classified according to the criteria of Inflammatory Bowel Disease Dysplasia Morphology Study Group.

Mad-homology (MH)1, intermediate linker, and MH2 domains.[13] Catalytically active TGF-β type I receptor (TβRI) phosphorylates the C-terminal serine residues of receptor-activated Smads,[14] which include Smad2 and the highly similar protein Smad3. The linker domain undergoes regulatory phosphorylation by Ras-associated kinases including c-Jun N-terminal kinase (JNK).[15–19] TβRI and Ras-associated kinases differentially phosphorylate Smad3 to create distinct phosphorylated forms: C-terminally phosphorylated Smad3 (pSmad3C), linker phosphorylated Smad3 (pSmad3L), and both linker and C-terminally phosphorylated Smad3 (pSmad3L/C).[20–23] Linker phosphorylation of Smad3 plays an important role in regulation of cytostatic pSmad3C signaling under both physiological and pathological conditions.[16–29] Phosphorylated Smad2 and Smad3 rapidly oligomerize with Smad4 and translocate to the nucleus, where they regulate transcription of target genes.[13]

During sporadic colorectal carcinogenesis, enterocytes affected by somatic mutations such as those involving the *K-ras* gene undergo transition from a tumor-suppressive pSmad3C pathway to an oncogenic pSmad3L pathway.[21,31] Our present studies extend the previous observations to UC-associated carcinogenesis. This investigation of Smad3 phosphorylation profiles in colitis, dysplasia, and cancer leads to the conclusion that additional oncogenic pSmad3L/C signaling induced by chronic inflammation is an important early event in UC-associated carcinogenesis.

MATERIALS AND METHODS

Colorectomy Specimens

According to the criteria of the Inflammatory Bowel Disease Dysplasia Morphology Study Group,[32] principal histologic features were evaluated independently by two pathologists with an interest in gastrointestinal neoplasia. Pathology records and histologic slides were obtained from the Department of Surgical Pathology at Keio University Hospital.

This study was approved by the Ethics Committee of Keio University. Tissue samples were obtained from colorectomy specimens from eight patients with UC who had undergone resections because of dysplasia and cancer (Table 1). Twelve specimens were prepared from normal colon tissue as a control group. UC patients included six men and two women with an age range of 28 to 60 years at diagnosis. The average duration of UC was 15.9 years (range, 9–22). Colorectal cancers included tumors classified histologically as well-differentiated adenocarcinoma ($n = 7$) and moderately differentiated adenocarcinoma ($n = 1$).

Domain-specific Antibodies (Abs) Against the Phosphorylated Smad3

Two polyclonal anti-phospho-Smad3 sera, α pSmad3L ($Ser^{208/213}$) and α pSmad3C ($Ser^{423/425}$), were raised against the phosphorylated linker and C-terminal regions of Smad3 by immunization of rabbits with synthetic peptides. Relevant antisera were affinity-purified using the phosphorylated peptides as described previously.[17]

Immunoprecipitation and Immunoblotting

HT-29 (human colonic epithelial cells) purchased from the American Type Culture Collection (Manassas, VA) were starved for 48 hours in serum-free medium and were treated with 20 pM TGF-β_1 (R&D Systems, Minneapolis, MN) and/or 400 pM tumor necrosis factor (TNF)-α (R&D Systems) for 30 minutes. To detect pSmad3L/C, nuclear extracts were immunoprecipitated with anti-pSmad3C antibody and the immunoprecipitates were immunoblotted using anti-pSmad3L antibody as described previously.[22]

Immunohistochemical and Immunofluorescence Analyses

Immunohistochemical and immunofluorescence studies were performed as described previously.[33] Primary Abs used in this study included mouse monoclonal anti-p53 antibody (Clone DO-7; dilution 1:50; Dako, Glostrup, Denmark), mouse monoclonal anti-c-Myc Ab (10 μg/mL; Santa Cruz Biotechnology, Santa Cruz, CA), and mouse monoclonal anti-$p21^{WAF1}$ Ab (0.5 μg/mL; Dako), in addition to the affinity-purified rabbit polyclonal anti-pSmad3L (2 μg/mL) and anti-pSmad3C (0.5 μg/mL) as described above. Anti-pSmad3C Ab crossreacted weakly with C-terminally phosphorylated Smad2: to block binding of anti-pSmad3C Ab to phosphorylated domains in Smad2, anti-pSmad3C Ab was adsorbed with 1 μg/mL C-terminally phosphorylated Smad2 peptide.

For immunohistochemical analyses, sections exposed to primary Abs were then incubated with peroxidase-labeled polymer conjugated to goat antimouse or antirabbit IgG (Dako). Finally, sections were developed with 3,3′-diaminobenzidine tetrahydrochloride (DAB; Vector Laboratories, Burlingame, CA), counterstained with Mayer's hematoxylin (Merck, Darmstadt, Germany), and mounted under coverslips.

For double-labeling immunofluorescence analyses, sections exposed to a pair of primary Abs (rabbit plus mouse) were then incubated in a 1:500 dilution of goat antirabbit IgG conjugated with a red fluorophore (Alexa Fluor 594; Molecular Probes, Eugene, OR) and goat antimouse IgG conjugated with a green fluorophore (Alexa Fluor 488; Molecular Probes). Images were obtained with a fluorescence microscope (Carl Zeiss Microimaging, Oberkochen, Germany).

Cells immunoreactive for p53, pSmad3L, and pSmad3C were counted among 1000 cells sampled from each of five randomly selected areas. The percentage of immunoreactive cells averaged between the five areas was defined as the immunostaining index (SI).

Polymerase Chain Reaction/Single Stranded Conformation Polymorphism (SSCP) and Polymerase Chain Reaction/Restriction Fragment Length Polymorphism (PCR-RFLP)

DNA extraction from paraffin-embedded/formalin-fixed tissue sections and isolation of PCR products were performed in accordance with the manufacturer's protocol (Takara, Shiga, Japan). Extracted DNA was amplified using PCR. We designed four pairs of primers to contain exons 5 to 8 of the p53 sequence.[34] To detect mutation of the *K-ras* gene, other primers were designed based on codon 12 sequence.[35] The primer sequences were: p53 forward (exon 5), 5′-TCTTCCTGCAGTACTCCCCT-3′; p53 reverse (exon 5), 5′-AGCTGCTCACCATCGCTATC-3′; p53 forward (exon 6), 5′-TGATTCCTCACTGATTGCTCT-3′; p53 reverse (exon 6), 5′-GAGACCCCAGTTGCAAACC-3′; p53 forward (exon 7), 5′-TTGTCTCCTAGGTTGGCTCT-3′; p53 reverse (exon 7), 5′-GCTCCTGACCTGGAG TCTTC-3′; p53 forward (exon 8), 5′-GCTTCTCTTTTCCT ATCCTGA-3′; p53 reverse (exon 8), 5′-CGCTTCTTGTC CTGCTTGC-3′; K-ras forward (codon 12), 5′-ACTGAATA TAAACTTGTGGTAGTTGGACCT-3′; K-ras reverse (codon 12), 5′-TCAAAGAATGGTCCTGGACC-3′.

Mutations of p53 exon 5 to 8 and K-ras codon 12 in amplified DNAs were investigated by SSCP and PCR-RFLP, respectively, as described previously.[34]

[^{3}H]thymidine Incorporation

DNA synthesis was measured by incorporation of 1 μCi/mL [^{3}H]thymidine (Amersham Pharmacia Biotech, Piscataway, NJ) into 5% trichloroacetic acid-precipitable material after a 4-hour pulse as described previously.[21]

Statistical Analyses

The luminal and basal portions of the normal crypts were statistically compared using the paired Student's *t*-test. Nonparametric Friedmann and Wilcoxon tests as repeated measures were used to identify significant differences in pSmad3L and pSmad3C positivities between colitis, dysplasia, and cancer. *P*-values less than 0.05 were considered significant.

RESULTS

Distribution of pSmad3L/c-Myc and pSmad3C/$p21^{WAF1}$ in Normal Colonic Crypts

Reversible shifting of Smad3-mediated signaling between tumor suppression and oncogenesis in hyperactive Ras-overexpressing epithelial cells indicates that the pSmad3C/$p21^{WAF1}$ pathway transmits a cytostatic TGF-β signal, while cell growth is promoted via the JNK-dependent pSmad3L/c-Myc pathway.[21] Linker phosphorylation of Smad3 indirectly inhibits its C-terminal phosphorylation, and subsequently suppresses the cytostatic pSmad3C signaling.[22] To investigate domain-specific phosphorylation in Smad3 signaling in vivo, we generated an Ab specific for each phosphorylation site to determine the distribution of pSmad3L and pSmad3C in normal human colonic crypts.

Normal intestinal specimens display a proliferative compartment consisting of actively growing enterocytes and a differentiated compartment consisting of apoptotic enterocytes. To assess proliferative versus cytostatic states in normal crypts, nuclear expression of c-Myc and $p21^{WAF1}$ was examined immunohistochemically. Immunoreactivity for pSmad3L showed a striking distribution,

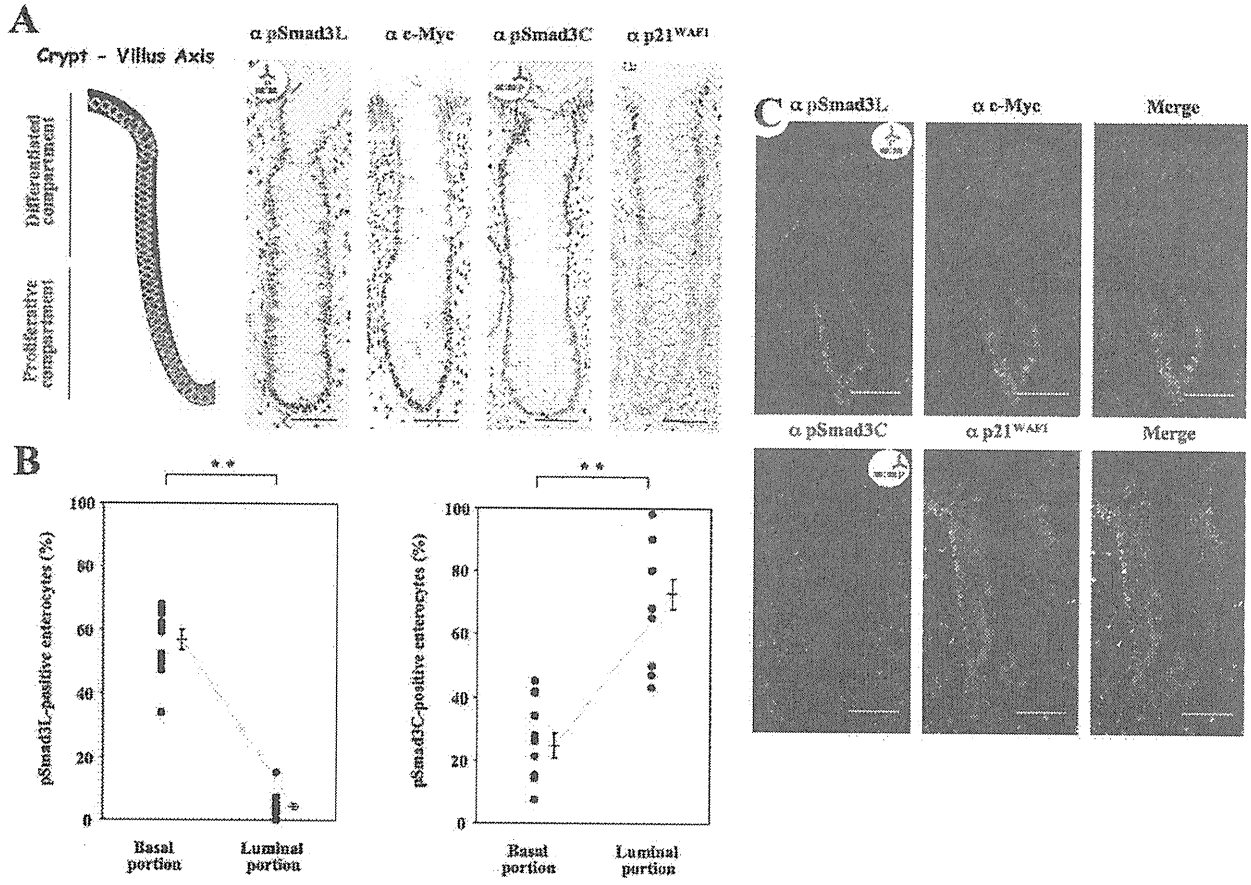

FIGURE 1. Physiological roles of pSmad3L and pSmad3C pathways in normal colonic crypts. (A) As enterocytes migrate upward from crypt base to villus, the pSmad3C/p21^{WAF1} pathway shows increasing prominence while the pSmad3L/c-Myc pathway decreases. Formalin-fixed, paraffin-embedded sections of normal colonic crypt were stained with anti-pSmad3L Ab (α pSmad3L column), anti-c-Myc Ab (α c-Myc column), anti-pSmad3C Ab (α pSmad3C column), or anti-p21^{WAF1} Ab (α p21^{WAF1} column). Sections stained for pSmad3L or pSmad3C were paired with an adjacent sections stained with anti-c-Myc Ab or anti-p21^{WAF1} Ab, respectively. Brown product indicates specific Ab reactivity. Scale bars = 100 μm. (B) Nuclei in the basal portion of normal crypts were stained with pSmad3L, whereas the differentiated compartment at the top of the crypts stained intensely with the antibody against pSmad3C. After staining, nuclear immunoreactive enterocytes were counted for calculation of percentage values (100 × positive cell counts/total cell counts), defined as the immunostaining index (SI). Immunoreactivity was evaluated by separating the luminal one-third and basal one-third of the normal crypts. The luminal and basal portions of the normal crypts were statistically compared using the paired Student's *t*-test. $^{**}P < 0.01$. (C) In normal crypt specimens, pSmad3L and pSmad3C in enterocytic nuclei colocalize with c-Myc and p21^{WAF1}, respectively. Sections of normal crypts were stained for immunofluorescence to simultaneously detect pSmad3L and pSmad3C (red), or c-Myc and p21^{WAF1} (green). Yellow color indicates overlap of proteins. The pSmad3L-immunoreactive enterocytes show c-Myc colocalization (upper row), while pSmad3C colocalize with p21^{WAF1} in other enterocytic nuclei (lower row). Scale bars = 100 μm. In parallel with the distribution of pSmad3L-immunoreactive enterocytes, c-Myc-immunoreactive enterocytes are confined to the proliferative compartments in the basal third of mucosal crypts (lower portions of crypts in α pSmad3L and α c-Myc columns). This staining declines in upper portions of the glands (differentiated compartments), becoming undetectable superficially (upper portions in α pSmad3L and α c-Myc columns). In contrast, pSmad3C is localized in the nuclei of p21^{WAF1}-immunoreactive mature enterocytes in differentiated compartments (upper portions in α pSmad3C and α p21^{WAF1} columns), while both pSmad3C and p21^{WAF1} are undetectable in proliferative compartments (lower portions in α pSmad3C and α p21^{WAF1} columns).

being present in the nuclei of c-Myc-immunoreactive progenitor cells at the bottom of mucosal crypts, representing the proliferative compartment (Fig. 1A, bottom portions of crypts in α pSmad3L and α c-Myc columns); this staining decreased in upper parts of crypts, which were populated by differentiated enterocytes. In particular, the superficial epithelium failed to show any phosphorylation at Smad3L. As enterocytes progressed upward to approach the

intestinal lumen, phosphorylation at Smad3C accompanied by $p21^{WAF1}$ expression increased in the nuclei of differentiated enterocytes (Fig. 1A, upper portions of crypts in α pSmad3C and α $p21^{WAF1}$ columns). We statistically compared the immunoreactivities in the upper and bottom portions of the normal crypts. pSmad3L was localized in the bottom one-third of normal crypts, whereas the differentiated compartment at the top one-third of the crypts stained intensely with the antibody against pSmad3C (Fig. 1B). Double-immunofluorescence studies in normal colonic crypt specimens confirmed that pSmad3L and pSmad3C colocalized with c-Myc and $p21^{WAF1}$, respectively (Fig. 1C). These findings suggest that normal progenitor cells located at the base of crypts might respond to pSmad3L-mediated signaling by proliferating, and then migrate upward.[21] In contrast, the pSmad3C pathway represents cytostatic functions such as growth inhibition and apoptosis.[13]

Oncogenic pSmad3L/C Signaling Induced by TGF-β and TNF-α in UC Specimens

Mounting evidence from preclinical and clinical studies suggests that persistent inflammation functions as a driving force toward development of colitic cancer.[5,36] TNF-α acts as a key factor mediating the immune response.[37] Serum concentrations of TGF-β and TNF-α are elevated in patients with UC.[38,39] These findings suggest that TNF-α can alter enterocytic TGF-β signaling in human UC.

We investigated this hypothesis using cultured human enterocytes. Before stimulation, the linker site of Smad3 was phosphorylated under basal conditions (Fig. 2A). However, the phosphorylation level was insignificant at the C-terminal regions of Smad3. TGF-β induced Smad3 phosphorylation at its C-terminal region. In contrast, TNF-α-dependent phosphorylation occurred on two serine residues within the linker region but not within the C-terminal region. Treatment of TNF-α together with TGF-β induced enterocytic Smad3 phosphorylation at both linker and C-terminal regions. Phospho-Smad3L immunoblotting of pSmad3C immunoprecipitates from nuclear extracts demonstrated that pSmad3L/C was localized in the nuclei of treated enterocytes. We further investigated whether TGF-β and/or TNF-α regulated DNA synthesis of the human enterocytes. Although TNF-α stimulated the enterocytic growth, TGF-β inhibited cell proliferation (Fig. 2B). Importantly, TGF-β enhanced the proliferative effect of TNF-α. Taken together, aberrant phosphorylation of Smad3L/C can lead to continuous enterocytic growth.[18,22]

We next investigated the relationship between pSmad3L/C and cellular proliferation in UC specimens. Figure 3A illustrates pSmad3L/C distribution and c-Myc/$p21^{WAF1}$ expression in a UC specimen from Patient 5 in Table 1. Throughout the glands in the specimen, Smad3 was phospho-

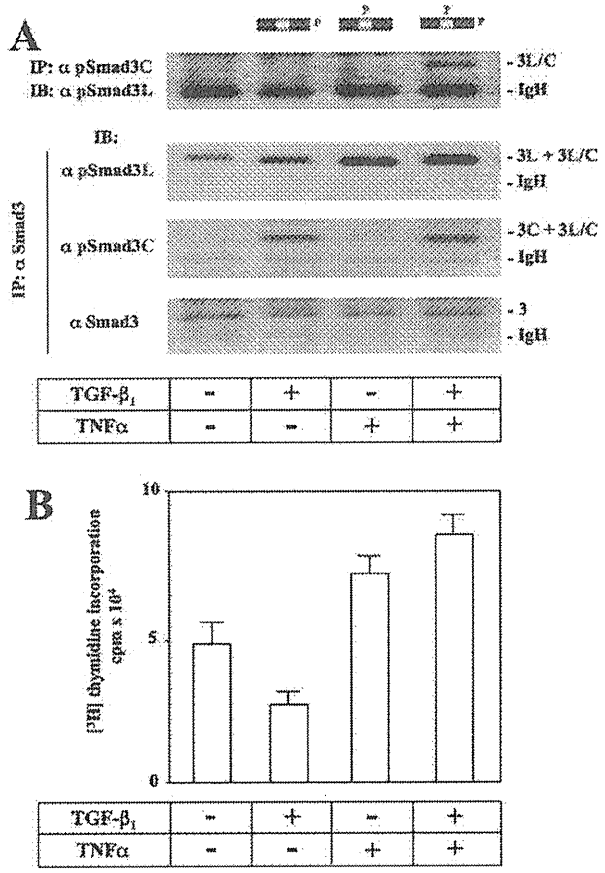

FIGURE 2. TNF-α in concert with TGF-β signaling converts Smad3 into pSmad3L/C, leading to colonic epithelial cell growth. (A) TNF-α together with TGF-β signaling converts Smad3 into pSmad3L/C. Serum-deprived human colonic epithelial cells were treated for 30 minutes with 20 pM TGF-β_1, 400 pM TNF-α, or a combination of both. To detect pSmad3L/C, nuclear extracts were immunoprecipitated (IP) with anti-pSmad3C antibody, and the immunoprecipitates were immunoblotted (IB) using anti-pSmad3L ($Ser^{208/213}$) antibody (upper panel). Following IP of nuclear extracts with anti-Smad3 antibody, phosphorylation of Smad3 was analyzed by IB as indicated (lower panels). (B) TNF-α together with TGF-β signaling stimulates enterocytic growth. Serum-deprived colonic epithelial cells (HT-29) were treated with 20 pM TGF-β_1, 400 pM TNF-α, or a combination of both for 20 hours followed by a 4-hour incubation with 1 μCi of [^{3}H] thymidine. The acid-insoluble [^{3}H] thymidine radioactivity was counted.

rylated at both linker and C-terminal regions. In parallel with the distribution of pSmad3L/C-immunoreactive enterocytes, c-Myc- but not $p21^{WAF1}$-immunoreactive enterocytes were evenly distributed throughout entire glands. Double-immunofluorescence studies confirmed pSmad3L/C to colocalize with c-Myc but not $p21^{WAF1}$ (Fig. 3B). These findings suggest that

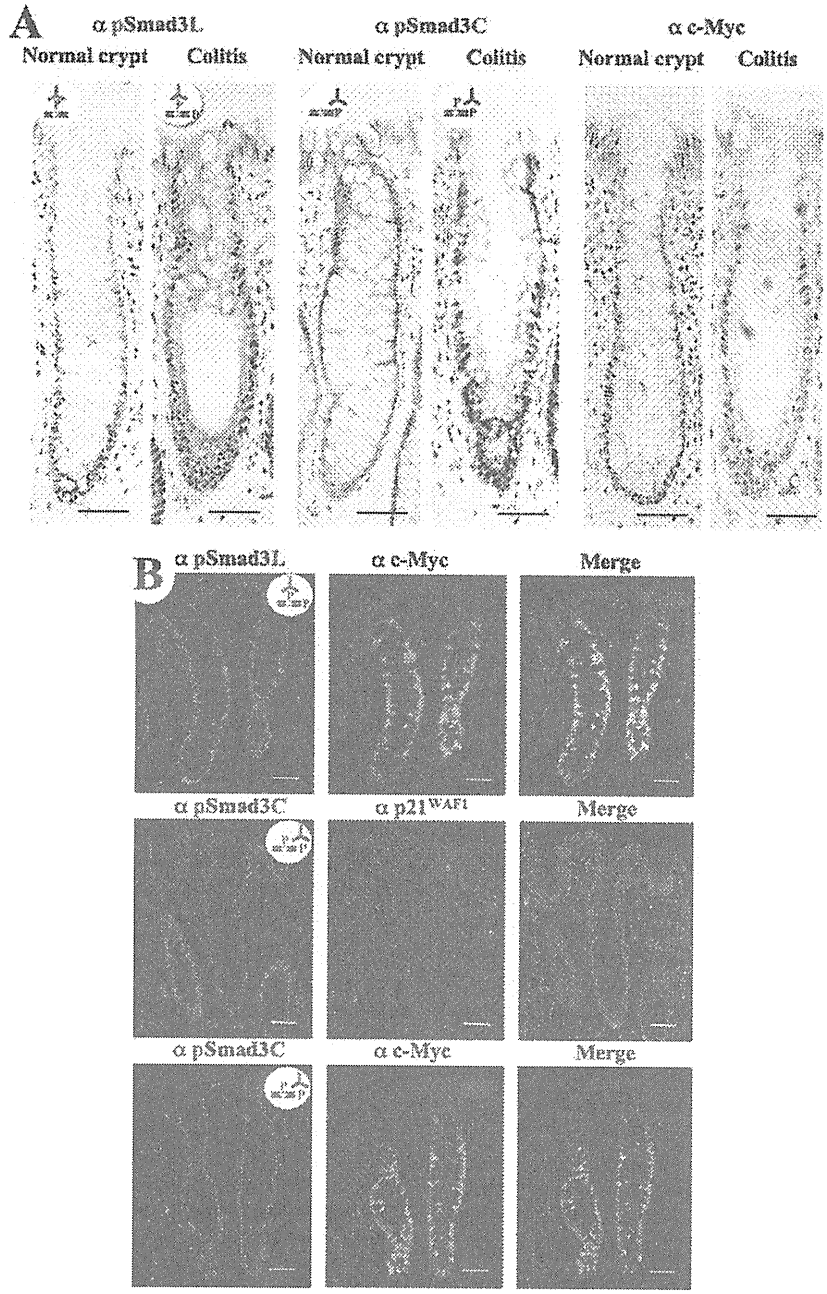

FIGURE 3. Smad3 is phosphorylated at both linker and C-terminal regions in the nuclei of c-Myc-immunoreactive enterocytes throughout the glands in UC lesions. (A) pSmad3L, pSmad3C, and c-Myc oncoprotein appear in the nuclei of affected enterocytes throughout the glands. Formalin-fixed, paraffin-embedded sections of colitis specimens were stained with anti-pSmad3L Ab (α pSmad3L column), anti-pSmad3C Ab (α pSmad3C column), or anti-c-Myc Ab (α c-Myc column). The section stained for c-Myc was paired with an adjacent section stained with anti-pSmad3L Ab or anti-pSmad3C Ab. Normal crypts were shown for comparison. Brown product indicates specific Ab reactivity. Scale bars = 100 μm. (B) In colitis specimens, nuclear pSmad3L/C colocalizes with c-Myc but not $p21^{WAF1}$. Sections of colitis tissues were stained for immunofluorescence to simultaneously detect pSmad3L/C (red), or c-Myc and $p21^{WAF1}$ (green). Yellow color indicates overlap of proteins. The pSmad3L/C-immunoreactive enterocytes show colocalization with c-Myc (top and bottom rows) but not $p21^{WAF1}$ (middle row). Scale bars = 100 μm.

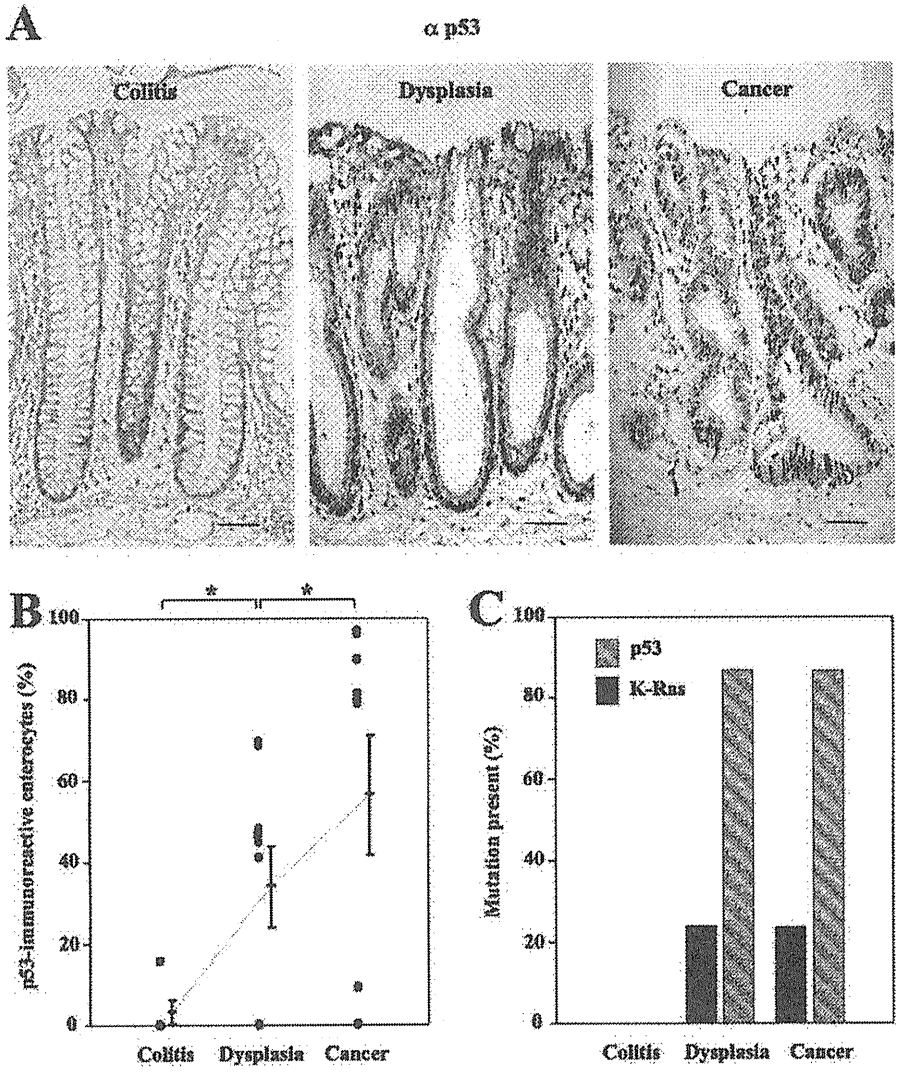

FIGURE 4. Nuclear accumulation of p53 protein and mutations of *p53* and *K-ras* genes in dysplastic and cancer specimens. (A) p53 protein appears in cell nuclei in dysplastic and cancer specimens. Formalin-fixed, paraffin-embedded sections of dysplastic and cancer specimens were stained with anti-p53 Ab (α p53 column). Brown product indicates specific Ab reactivity. Scale bars = 100 μm. (B) p53-immunoreactive enterocytes increase as UC-associated chronic colorectal disorders progress. The p53 protein in cell nuclei in dysplasia and cancer is significantly more abundant than in enterocytic nuclei in colitis specimens. Percentage of p53-immunoreactive enterocytes was calculated. *$P < 0.05$. (C) Mutations of *p53* and *K-ras* genes were detectable only in dysplastic and cancer specimens. The percentage of mutation frequencies in colitis, dysplasia, and cancer specimens was calculated.

enterocytes affected by chronic inflammation retain a proliferative phenotype throughout the glands.

Nuclear Accumulation of p53 Protein and Mutations of p53 and K-ras Genes in Specimens Representing Dysplasia and Cancer

Mutations of *p53* and *K-ras* genes represent two important genetic abnormalities in UC-associated neoplasms, leading us to analyze mutations of these genes in eight samples containing dysplasia and cancer. Enterocytes immunoreactive for p53 increased as UC-associated chronic colonic disorders progressed (Fig. 4A). Five of eight dysplasia samples and six of eight cancer samples showed p53 positivity, but only one of eight colitis samples showed staining for p53 protein (Fig. 4B; 62.5% and 75% versus 12.5%, $P < 0.05$). When PCR products from tissue samples were

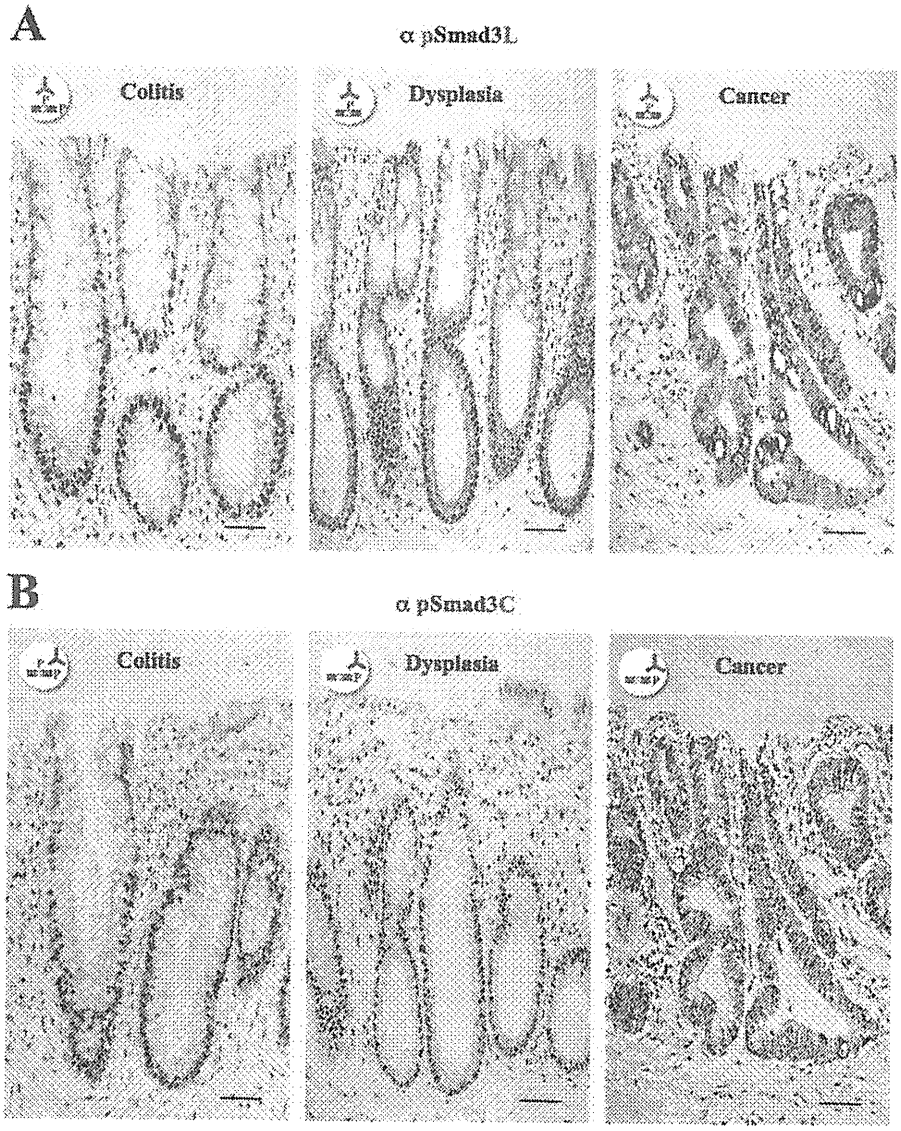

FIGURE 5. As UC-associated carcinogenesis progresses from colitis through dysplasia to cancer, the pSmad3L/c-Myc pathway shows increasing prominence while the pSmad3C/p21^{WAF1} pathway becomes less active. (A,B) The pSmad3L pathway shows increasing prominence, while the pSmad3C pathway becomes less evident as UC-associated carcinogenesis progresses. Formalin-fixed, paraffin-embedded sections showing colitis, dysplasia, and cancer were stained with anti-pSmad3L Ab (A; α pSmad3L column), or anti-pSmad3C Ab (B; α pSmad3C column). A section stained for pSmad3L was paired with an adjacent section stained with anti-pSmad3C Ab. Brown product indicates specific Ab reactivity. Scale bars = 100 μm. (C,D) pSmad3L in cell nuclei in dysplastic and cancer specimens colocalizes with c-Myc. Colon sections showing dysplasia (C) and cancer (D) were stained for immunofluorescence to simultaneously detect pSmad3L and pSmad3C (red), or c-Myc and p21^{WAF1} (green). Yellow color indicates overlap of proteins. Cells immunoreactive for pSmad3L show c-Myc colocalization (upper rows), while pSmad3C and p21^{WAF1} are undetectable in cell nuclei (lower rows). Scale bars = 100 μm.

analyzed by SSCP and PCR-RFLP, we detected mutations of *p53* and *K-ras* genes only in dysplastic or cancer specimens. Seven of eight dysplastic samples and seven of eight cancer samples showed *p53* mutation (Fig. 4C; 87.5% for each), while *K-ras* mutation was detected in two of eight dysplastic samples and two of eight cancer samples (Fig. 4C; 25.0% for each). No mutations of *p53* or *K-ras* genes were detected in colitis samples.

As UC-associated carcinogenesis progresses from colitis through dysplasia to cancer, the pSmad3L/c-Myc

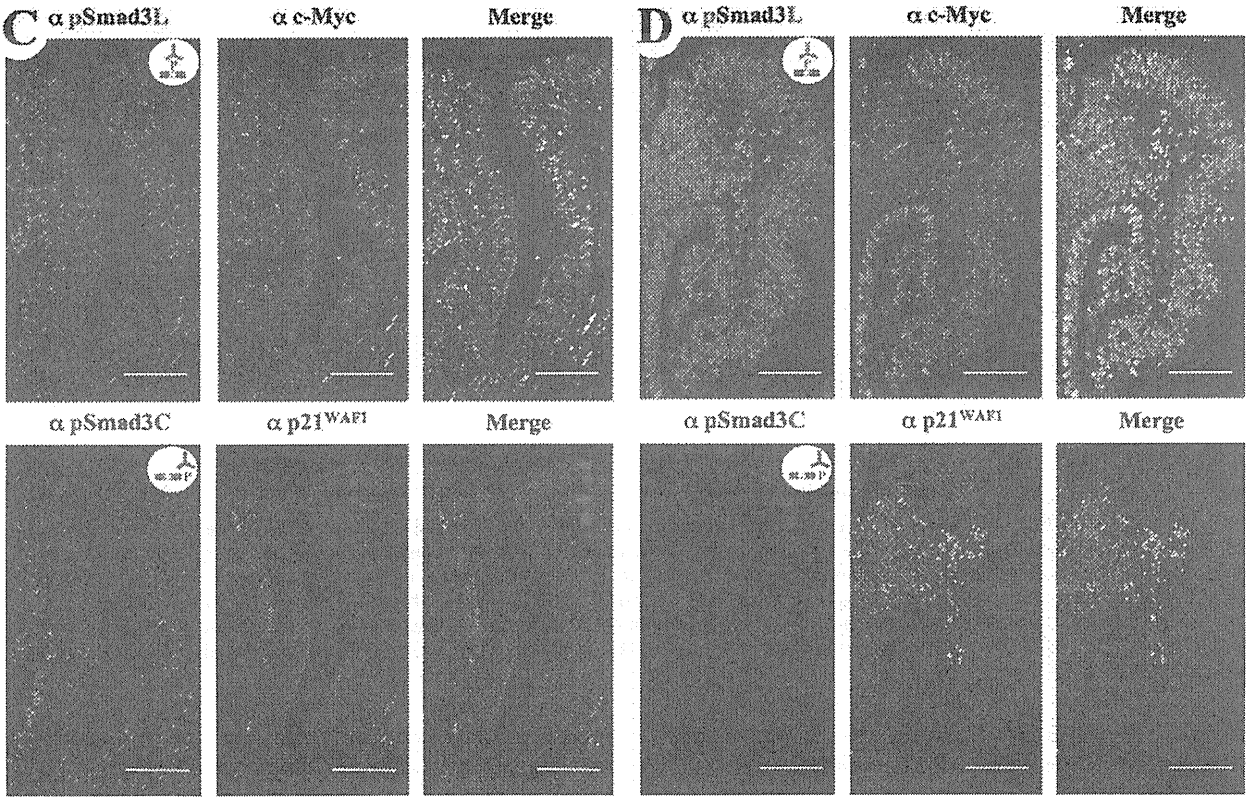

FIGURE 5. (Continued)

pathway shows increasing prominence, while the pSmad3C/$p21^{WAF1}$ pathway decreases.

Finally, we investigated the distribution of Smad3 phosphoisoforms in human UC, dysplasia, and cancer from Patient 7 in Table 1 (Fig. 5A,B). Immunostaining with Abs against Smad3 at linker or C-terminal regions indicated that Smad3 in enterocytes of UC specimens was phosphorylated at both linker and C-terminal regions, and that pSmad3L/C was localized predominantly in nuclei (Fig. 5A,B, colitis panels). Throughout glands present in dysplasia and cancer, pSmad3L was significantly more abundant than that in enterocytes of colitic specimens (Fig. 5A, dysplasia and cancer panels). Glands showing highly phosphorylated Smad3L were uniformly distributed in nuclei of dyslastic and cancer cells. In contrast to highly phosphorylated states for Smad3L, Smad3C showed little phosphorylation in cancer (Fig. 5B, cancer panel). Degrees of phosphorylation at Smad3C in dysplasia were intermediate between those in UC and cancer (Fig. 5B, dysplasia panel). Double-immunofluorescence studies confirmed positive relationships between pSmad3L distribution and c-Myc expression in dysplastic and cancer specimens (Fig. 5C,D). Throughout cancer glands, pSmad3L/c-Myc was significantly more abundant than in dysplastic glands (upper rows in Fig. 5D versus 5C). Glands showing highly phosphorylated Smad3L accompanied by c-Myc expression were evenly distributed in cancers (Fig. 5D, upper rows). In actively growing c-Myc-immunoreactive cancers, pSmad3L was localized exclusively in cell nuclei. When we quantified extent of phosphorylation at Smad3L and Smad3C by counting pSmad3L- and pSmad3C-immunoreactive enterocytes, upregulation of pSmad3L was seen, while pSmad3C gradually decreased as colonic carcinogenesis progressed (Fig. 6). Taking these observations together, the oncogenic pSmad3L pathway in enterocytes comes to predominate while the tumor-suppressive pSmad3C pathway becomes quiescent as UC progresses to dysplasia and then cancer.

DISCUSSION

Formation of colitic cancer is a complex stepwise process involving alteration of the physiological Smad3 signaling shown in normal colonic crypts. UC-associated carcinogenesis represents a multifactorial collaboration between two or more agents promoting colitic cancer

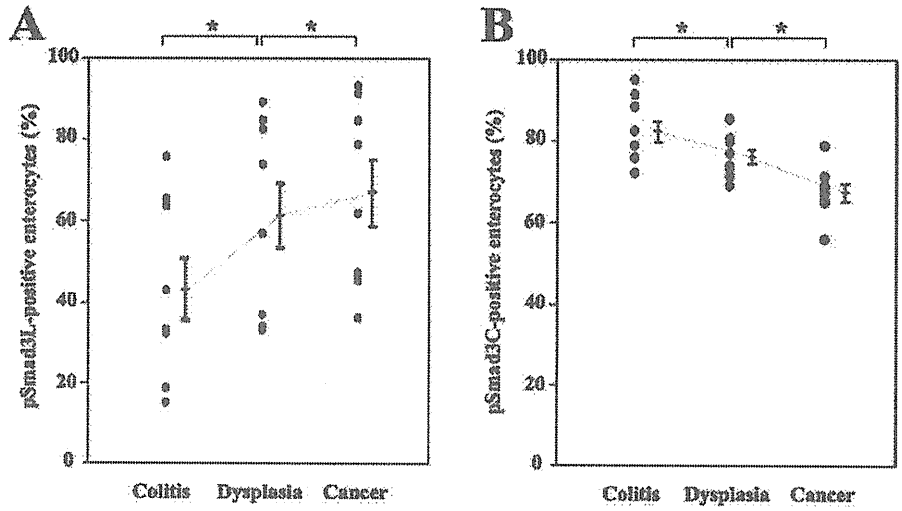

FIGURE 6. UC-associated carcinogenesis: reciprocal change in pSmad3L and pSmad3C pathways. (A) Enterocytic phosphorylation at Smad3L increases as UC-associated chronic colonic disorders progress. Phosphorylation at Smad3L in cell nuclei of dysplastic and cancer specimens is significantly greater than in enterocytic nuclei of colitic specimens. The percentage of pSmad3L-immunoreactive enterocytes was calculated. $^*P < 0.05$. (B) Enterocytic phosphorylation at Smad3C decreases as UC-associated chronic colonic disorders progress. Phosphorylation at Smad3C in cell nuclei of dysplastic and cancer specimens is lower than in enterocytic nuclei of colitic specimens. The percentage of pSmad3C-immunoreactive enterocytes was calculated. $^*P < 0.05$.

occurrence. Among these influences, chronic inflammation and somatic mutations appear mainly responsible for colitic cancer pathogenesis.[5,8–10] Differences in morphology and biological behavior between sporadic colorectal cancer and colitic cancer raise an important question of how chronic inflammation contributes to development of colitic cancer. Our current study therefore examined the differential roles of pSmad3L, pSmad3C, and pSmad3L/C signaling during UC-associated carcinogenesis.

Physiological Roles of pSmad3L and pSmad3C Pathway in Normal Colonic Crypts

In the colon, enterocytes are constantly renewed by immature cells proliferating at the base of mucosal crypts and are migrating upward to the luminal surface. This process is tightly controlled by a delicate balance between proliferation and differentiation of enterocytes. The phosphorylation pattern of Smad3 in normal colonic mucosa suggests the importance of Smad3 in maintaining this balance. In immature enterocytes near the bottom of normal colonic crypts, intracellular phosphorylation at Smad3L is high (Fig. 1). Translocated to the nucleus, pSmad3L stimulates c-Myc transcription; this increases proliferation of enterocytes[21] and opposes the cytostatic action of the pSmad3C/p21^{WAF1} pathway.[22] Accordingly, pSmad3C was undetectable at the bottom of normal crypts: escape from TGF-β-induced cytostasis is crucial in a subset of progenitor cells devoted to ensuring epithelial renewal.[13] As the enterocytes approach the lumen and phosphorylation at Smad3L decreases, cell proliferation ceases. Since decreased pSmad3L can lead to increased sensitivity to phosphorylation at Smad3C by TβRI,[21] mature enterocytes stop their growth and ultimately begin the process of apoptosis via the cytostatic pSmad3C pathway (Fig. 7A, left).[40] This entire process of outmigration and cell death takes only 3 to 4 days.

Continuous Phosphorylation at Smad3L/C in Colitis: A Primary Event in UC-associated Carcinogenesis

In UC specimens the normal balance between proliferation and differentiation in colonic crypts is lost. Chronic inflammation stimulates the enterocytes to proliferate continuously in an organ that normally experiences it hardly at all: proliferation by the progenitor cells is tightly regulated by the cytostatic pSmad3C signaling (Fig. 7A, left). Such signaling represents a highly effective defense mechanism against development of colitic cancer, since almost all enterocytes positive for pSmad3C that sustain any mutations are destined to die. TNF-α induced by chronic inflammation can alter TGF-β signaling to form pSmad3L/C in the affected enterocytic nuclei (Fig. 2). If pSmad3L/C-positive enterocytes persist over decades throughout the mucosa in colitis and proliferate by continuous upregulation of c-Myc oncoprotein (Fig. 7A, right),[41] as opposed to the pSmad3C-immunoreactive enterocytes shown by normal

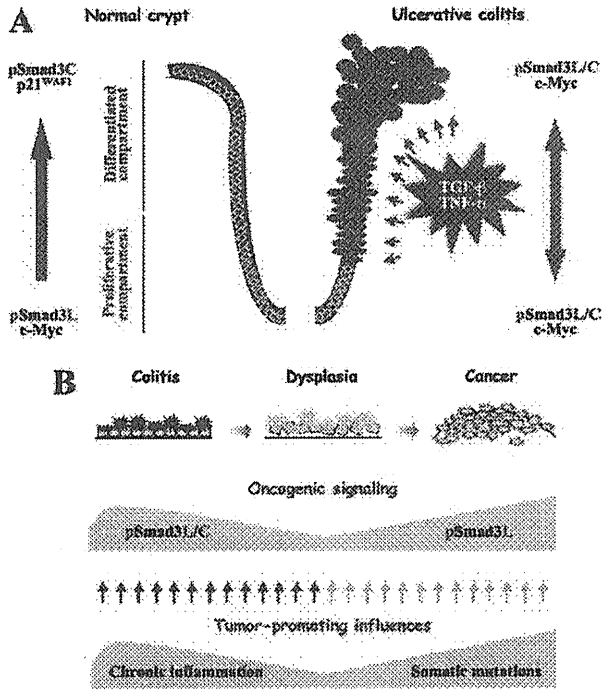

FIGURE 7. Oncogenic pSmad3L/C signaling induced by chronic inflammation can promote somatic mutations, which in turn activate another oncogenic pathway, pSmad3L. (A) Chronic inflammation is a primary initial event in UC-associated multistep carcinogenesis. Left, as enterocytes migrate upward toward the lumen with arrest of proliferation and ultimate apoptosis, the cytostatic pSmad3C/$p21^{WAF1}$ pathway tends to increase in activity with suppression of the pSmad3L/c-Myc pathway. Right, if enterocytes are exposed to TGF-β and TNF-α over decades of UC and pSmad3L/C-positive enterocytes persist in colitic tissues, the affected enterocytes can accumulate mutant alleles and pass them on to their descendants. (B) During later stages of the oncogenic process, somatic mutations such as those involving *p53* and *K-ras* genes can drive to full malignancy by activating the oncogenic pSmad3L pathway.

colonic lumen, enterocytes affected by UC might accumulate mutant alleles and pass them on to their descendants.

Somatic Mutations in Dysplasia and Cancer as Promoters of Oncogenic pSmad3L Signaling and Inhibitors of Tumor-suppressive pSmad3C Signaling

Somatic mutations in dysplasia can include changes in *p53* and *K-ras* genes (Fig. 4) that favor progression of dysplasia to cancer.[42,43] Although the causal relationship between *p53* mutations and pSmad3L remains largely unknown, pSmad3L can accumulate in nuclei of dysplastic enterocytes because of Ras mutations that activate the JNK pathway to phosphorylate Smad3 at the linker region.[21] More specifically, the proliferative effect mediated via the JNK/pSmad3L pathway antagonizes TGF-β signaling via the growth-inhibitory pSmad3C pathway in mature enterocytes (Fig. 1).[22] Accordingly, pSmad3L/c-Myc oncogenic signaling in enterocytes comes to predominate while the tumor-suppressive pSmad3C/$p21^{WAF1}$ pathway becomes quiescent as colitis progresses to dysplasia and then cancer. Constitutively phosphorylated Smad3L is likely to blunt pSmad3C-dependent cytostatic effects.[21] Some tumor-promoting effects of pSmad3L involve its ability to indirectly protect enterocytes from apoptosis via the pSmad3C pathway.[21] Escaping the cytostatic action of pSmad3C is a critical step for progression to full malignancy in cancers, which overcomes multiple fail-safe genetic controls.[40]

Similarities and Differences in Oncogenic Smad3 Signaling Between UC-associated and Sporadic Colorectal Carcinogenesis

Oncogenic Smad3 signaling shows both similarities and differences between UC-associated and sporadic colorectal carcinogenesis.

In early stages of UC-associated and sporadic colorectal carcinogenesis, chronic inflammation and somatic mutations are independently associated with Smad3-mediated signals initiating cancer development. UC specimens show intense pSmad3L/C immunostaining in nuclei of all enterocytes throughout entire glands (Fig. 3). In contrast, pSmad3L/C induced by chronic inflammation rarely exists in the adenomas that can give rise to sporadic colonic cancers.[31] When pSmad3L/C is detected in sporadic colorectal cancers, the lesions are advanced with distant metastases.[22] Thus, chronic inflammation in UC can trigger the oncogenic pSmad3L/C pathway.

Like sporadic colorectal cancer, colitic cancer is a consequence of accumulated somatic genetic mutations. Emerging evidence suggests that frequencies of chromosomal instability (85%) and microsatellite instability (15%) in colitic cancer are roughly the same as in sporadic colorectal cancer.[8–10] During the later stages of the oncogenic process in both sporadic and colitic cancer, somatic mutations in human cancer development can be explained in terms of Smad3 signal transduction. As seen in the later stages of sporadic colorectal carcinogenesis, strong pSmad3L but weak pSmad3C positivities are observed in cell nuclei in UC-associated dysplasia and carcinoma (Figs. 5, 6).[31] Somatic mutations commonly found in association with these two oncogenic steps might accelerate oncogenic pSmad3L signaling while downregulating tumor-suppressing pSmad3C signaling, leading to a highly carcinogenic state.

CONCLUSIONS AND PERSPECTIVES

Both chronic inflammation and somatic mutations likely contribute to the pathogenesis of colitic cancers,

which frequently afflict individuals with long-standing UC. Our current data support a multistep model of tumor formation that involves an initial increase of enterocytic pSmad3L/C, possibly as a result of chronic inflammation in UC. Later, dysplastic enterocytes acquire somatic mutations that induce the oncogenic pSmad3L signaling. Our current data provide a new view of chronic inflammation and somatic mutations cooperating to promote cancer progression by upregulating a growth-related protein (Fig. 7B).

Chemoprevention of colitic cancer is an area of great interest and intense investigation. Evidence is accumulating that 5-aminosalicylic acid compounds may prevent development of colitic cancer by reducing chronic inflammation.[7,44] Selective blockade of linker phosphorylation abolishes the oncogenic pSmad3L/C and pSmad3L signals, while restoring the lost tumor-suppressive pSmad3C signaling shown by normal epithelial cells.[45] In evaluating the likely benefit from therapy against UC, domain-specific phosphorylation of Smad3 should serve as a useful biomarker.

REFERENCES

1. Eaden JA, Abrams KR, Mayberry JF. The risk of colorectal cancer in ulcerative colitis: a meta-analysis. *Gut.* 2001;48:526–535.
2. Ekbom A, Helmick C, Zack M, et al. Ulcerative colitis and colorectal cancer. A population-based study. *N Engl J Med.* 1990;323: 1228–1233.
3. Riddell RH. Dysplasia in inflammatory bowel disease. *Clin Gastroenterol.* 1980;9:439–458.
4. Dobbins WO III. Dysplasia and malignancy in inflammatory bowel disease. *Annu Rev Med.* 1984;35:33–48.
5. Itzkowitz SH, Yio X. Inflammation and cancer. IV. Colorectal cancer in inflammatory bowel disease: the role of inflammation. *Am J Physiol Gastrointest Liver Physiol.* 2004;287:G7–G17.
6. Rutter M, Saunders B, Wilkinson K, et al. Severity of inflammation is a risk factor for colorectal neoplasia in ulcerative colitis. *Gastroenterology.* 2004;126:451–459.
7. Velayos FS, Terdiman JP, Walsh JM. Effect of 5-aminosalicylate use on colorectal cancer and dysplasia risk: a systematic review and meta-analysis of observational studies. *Am J Gastroenterol.* 2005;100: 1345–1353.
8. Rabinovitch PS, Dziadon S, Brentnall TA, et al. Pancolonic chromosomal instability precedes dysplasia and cancer in ulcerative colitis. *Cancer Res.* 1999;59:5148–5153.
9. Brentnall TA, Crispin DA, Bronner MP, et al. Microsatellite instability in nonneoplastic mucosa from patients with chronic ulcerative colitis. *Cancer Res.* 1996;56:1237–1240.
10. Willenbucher RF, Aust DE, Chang CG, et al. Genomic instability is an early event during the progression pathway of ulcerative-colitis-related neoplasia. *Am J Pathol.* 1999;154:1825–1830.
11. Roberts AB, Sporn MB. The transforming growth factor-βs. In: Sporn MB, Roberts AB, eds. Peptide Growth Factors and Their Receptors. Berlin: Springer; 1990. p 419–472.
12. Heldin CH, Miyazono K, ten Dijke P. TGF-β signaling from cell membrane to nucleus through SMAD proteins. *Nature.* 1997;390: 465–471.
13. Massagué J. TGF-β signal transduction. *Annu Rev Biochem.* 1998;67: 753–791.
14. Wrana JL. Regulation of Smad activity. *Cell.* 2000;100:189–192.
15. Kretzschmar M, Doody J, Timokhina I, et al. A mechanism of repression of TGF-β/Smad signaling by oncogenic Ras. *Genes Dev.* 1999; 13:804–816.
16. Mori S, Matsuzaki K, Yoshida K, et al. TGF-β and HGF transmit the signals through JNK-dependent Smad2/3 phosphorylation at the linker regions. *Oncogene.* 2004;23:7416–7429.
17. Furukawa F, Matsuzaki K, Mori S, et al. p38 MAPK mediates fibrogenic signal through Smad3 phosphorylation in rat myofibroblasts. *Hepatology.* 2003;38:879–889.
18. Matsuura I, Denissova NG, Wang G, et al. Cyclin-dependent kinases regulate the antiproliferative function of Smads. *Nature.* 2004;430: 226–231.
19. Millet C, Yamashita M, Heller M, et al. A negative feedback control of transforming growth factor-β signaling by glycogen synthase kinase 3-mediated Smad3 Linker phosphorylation at Ser-204. *J Biol Chem.* 2009;284:19808–19816.
20. Matsuzaki K. Smad3 phosphoisoform-mediated signaling during sporadic human colorectal carcinogenesis. *Histol Histopathol.* 2006;21: 645–662.
21. Sekimoto G, Matsuzaki K, Yoshida K, et al. Reversible Smad-dependent signaling between tumor suppression and oncogenesis. *Cancer Res.* 2007;67:5090–5096.
22. Matsuzaki K, Kitano C, Murata M, et al. Smad2 and Smad3 phosphorylated at both linker and COOH-terminal regions transmit malignant TGF-β signal in later stages of human colorectal cancer. *Cancer Res.* 2009;69:5321–5330.
23. Alarcón C, Zaromytidou AI, Xi Q, et al. Nuclear CDKs drive Smad transcriptional activation and turnover in BMP and TGF-β pathways. *Cell.* 2009;139:757–769.
24. Wrighton KH, Lin X, Feng XH. Phospho-control of TGF-β superfamily signaling. *Cell Res.* 2009;19:8–20.
25. Guo X, Wang XF. Signaling cross-talk between TGF-β/BMP and other pathways. *Cell Res.* 2009;19:71–88.
26. Wang G, Matsuura I, He D, et al. Transforming growth factor-β-inducible phosphorylation of Smad3. *J Biol Chem.* 2009;284:9663–9673.
27. Chen D, Lin Q, Box N, et al. SKI knockdown inhibits human melanoma tumor growth in vivo. *Pigment Cell Melanoma Res.* 2009;22: 761–772.
28. Hamajima H, Ozaki I, Zhang H, et al. Modulation of the transforming growth factor-β1-induced Smad phosphorylation by the extracellular matrix receptor beta1-integrin. *Int J Oncol.* 2009;35:1441–1447.
29. Matsuura I, Chiang KN, Lai CY, et al. Pin1 promotes transforming growth factor-β-induced migration and invasion. *J Biol Chem.* 2010; 285:1754–1764.
30. Derynck R, Zhang YE. Smad-dependent and Smad-independent pathways in TGF-β family signaling. *Nature.* 2003;425:577–584.
31. Yamagata H, Matsuzaki K, Mori S, et al. Acceleration of Smad2 and Smad3 phosphorylation via c-Jun NH(2)-terminal kinase during human colorectal carcinogenesis. *Cancer Res.* 2005;65:157–165.
32. Riddell RH, Goldman H, Ransohoff DF, et al. Dysplasia in inflammatory bowel disease: standardized classification with provisional clinical applications. *Hum Pathol.* 1983;14:931–968.
33. Murata M, Matsuzaki K, Yoshida K, et al. Hepatitis B virus X protein shifts human hepatic TGF-β signaling from tumor-suppression to oncogenesis in early chronic hepatitis B. *Hepatology.* 2009;49: 1203–1217.
34. Fujii S, Fujimori T, Chiba T. Usefulness of analysis of p53 alteration and observation of surface microstructure for diagnosis of ulcerative colitis-associated colorectal neoplasia. *J Exp Clin Cancer Res.* 2003; 22:107–115.
35. Jiang W, Kahn SM, Guillem JG, et al. Rapid detection of ras oncogenes in human tumors: applications to colon, esophageal, and gastric cancer. *Oncogene.* 1989;4:923–928
36. Lin WW, Karin M. A cytokine-mediated link between innate immunity, inflammation, and cancer. *J Clin Invest.* 2007;117:1175–1183.
37. Papadakis KA, Targan SR. Role of cytokines in the pathogenesis of inflammatory bowel disease. *Annu Rev Med.* 2000;51:289–298.
38. Murch SH, Lamkin VA, Savage MO, et al. Serum concentrations of tumor necrosis factor α in childhood chronic inflammatory bowel disease. *Gut.* 1991;32:913–917.
39. Wiercińska-Drapało A, Flisiak R, Prokopowicz D. Effect of ulcerative colitis activity on plasma concentration of transforming growth factor β1. *Cytokine.* 2001;14:343–346.

40. Yang YA, Zhang GM, Feigenbaum L, et al. Smad3 reduces susceptibility to hepatocarcinoma by sensitizing hepatocytes to apoptosis through downregulation of Bcl-2. *Cancer Cell.* 2006;9:445–457.
41. Macpherson AJ, Chester KA, Robson L, et al. Increased expression of c-myc proto-oncogene in biopsies of ulcerative colitis and Crohn's colitis. *Gut.* 1992;33:651–656.
42. Chaubert P, Benhattar J, Saraga E, et al. K-ras mutations and p53 alterations in neoplastic and nonneoplastic lesions associated with long-standing ulcerative colitis. *Am J Pathol.* 1994;144:767–775.
43. Holzmann K, Klump B, Borchard F, et al. Comparative analysis of histology, DNA content, p53 and Ki-ras mutations in colectomy specimens with long-standing ulcerative colitis. *Int J Cancer.* 1998;76:1–6.
44. Ikeda I, Tomimoto A, Wada K, et al. 5-Aminosalicylic acid given in the remission stage of colitis suppresses colitis-associated cancer in a mouse colitis model. *Clin Cancer Res.* 2007;13:6527–6531.
45. Nagata H, Hatano E, Tada M, et al. Inhibition of c-Jun NH2-terminal kinase switches Smad3 signaling from oncogenesis to tumor-suppression in rat hepatocellular carcinoma. *Hepatology.* 2009;49:1944–1953.

Suppression of *Hath1* Gene Expression Directly Regulated by Hes1 Via Notch Signaling Is Associated with Goblet Cell Depletion in Ulcerative Colitis

Xiu Zheng, MD, Kiichiro Tsuchiya, MD, PhD, Ryuichi Okamoto, MD, PhD, Michiko Iwasaki, MD, PhD, Yoshihito Kano, MD, Naoya Sakamoto, MD, PhD, Tetsuya Nakamura, MD, PhD, and Mamoru Watanabe, MD, PhD

Background: The transcription factor *Atoh1/Hath1* plays crucial roles in the differentiation program of human intestinal epithelium cells (IECs). Although previous studies have indicated that the Notch signal suppresses the differentiation program of IEC, the mechanism by which it does so remains unknown. This study shows that the undifferentiated state is maintained by the suppression of the *Hath1* gene in human intestine.

Methods: To assess the effect of Notch signaling, doxycycline-induced expression of Notch intracellular domain (NICD) and Hes1 cells were generated in LS174T. *Hath1* gene expression was analyzed by quantitative reverse-transcription polymerase chain reaction (RT-PCR). Hath1 promoter region targeted by HES1 was determined by both reporter analysis and ChIP assay. Expression of Hath1 protein in ulcerative colitis (UC) was examined by immunohistochemistry.

Results: Hath1 mRNA expression was increased by Notch signal inhibition. However, Hath1 expression was suppressed by ectopic HES1 expression alone even under Notch signal inhibition. Suppression of the *Hath1* gene by Hes1, which binds to the 5′ promoter region of Hath1, resulted in suppression of the phenotypic gene expression for goblet cells. In UC, the cooperation of aberrant expression of HES1 and the disappearance of caudal type homeobox 2 (CDX2) caused Hath1 suppression, resulting in goblet cell depletion.

Conclusions: The present study suggests that Hes1 is essential for *Hath1* gene suppression via Notch signaling. Moreover, the suppression of Hath1 is associated with goblet cell depletion in UC. Understanding the regulation of goblet cell depletion may lead to the development of new therapy for UC.

(Inflamm Bowel Dis 2011;000:000–000)

Key Words: ulcerative colitis, Hath1, Hes1, Notch signaling

The gut epithelium undergoes continual renewal throughout adult life, maintaining the proper architecture and function of the intestinal crypts. This process involves highly coordinated regulation of the induction of cellular differentiation and the cessation of proliferation, and vice versa.[1–3] Many studies of the regulation of intestinal differentiation have shown that cellular formation of the villi in small and large intestine is affected by various intracellular signaling pathways such as Notch, Wnt, and BMP.[4–7] Moreover, recent studies have also shown that dysregulation of the differentiation system for prompt intestinal epithelial cell formation induces the pathology of such intestinal diseases as colon cancer, Crohn's disease and ulcerative colitis (UC).[8] Then it was suggested that crucial genes for the differentiation of intestinal epithelium cells (IECs) become corrupt by aberrant cell signaling on the pathogenesis of intestinal diseases.

One of the most important genes for cell formation is a basic helix-loop-helix (bHLH) transcription factor, *Atoh1*, and its human homolog, *Hath1*, which is essential for the differentiation toward secretory lineages in small and large intestine.[9] Using a ubiquitin proteasomal system, we demonstrated that regulation of Hath1 protein in colon carcinogenesis is regulated by glycogen synthase kinase 3β (GSK3β) via Wnt signaling. Moreover, Hath1 and β-catenin protein are reciprocally regulated by GSK3β in Wnt signaling for the coordination between cell differentiation and

Additional Supporting Information may be found in the online version of this article.

Received for publication November 9, 2010; Accepted November 15, 2010.

From the Department of Gastroenterology and Hepatology, Graduate School, Tokyo Medical and Dental University, Tokyo, Japan.

Supported in part by grants-in-aid for Scientific Research 19209027, 21590803, 21790651, and 21790653, from the Japanese Ministry of Education, Culture, Sports, Science and Technology; JFE (Japanese Foundation for Research and Promotion of Endoscopy); Japan Foundation for Applied Enzymology; Intractable Diseases, the Health and Labor Sciences Research Grants from the Japanese Ministry of Health, Labor and Welfare.

The first two authors contributed equally to this work.

Reprints: Mamoru Watanabe, MD, PhD, MD, PhD, Professor and Chairman, Department of Gastroenterology and Hepatology, Graduate School, Tokyo Medical and Dental University, 1-5-45 Yushima, Bunkyo-ku, Tokyo 113-8519, Japan (e-mail: mamoru.gast@tmd.ac.jp)

DOI 10.1002/ibd.21611

Published online 00 Month 2011 in Wiley Online Library (wileyonlinelibrary.com).

proliferation. These findings together indicate that the deletion of adenomatous polyposis coli (APC) in colon carcinogenesis causes Hath1 protein degradation by switching the target of GSK3β from β-catenin to Hath1, resulting in maintenance of the undifferentiated state.[10] The dysregulation of prompt differentiation of IEC thus causes major intestinal diseases, and elucidation of the roles of various cell-signaling pathways in intestine is therefore important in understanding the pathogenesis of intestinal diseases.

We have also recently reported aberrant expression of Notch intracellular domain (NICD) in lesions showing goblet cell depletion in UC patients.[8] Moreover, forced expression of NICD caused the suppression of phenotypic genes for goblet cells in human intestinal epithelial cells. It has also been reported that forced expression of NICD in murine intestinal epithelial cells caused the depletion of goblet cells with the decrease of Atoh1 expression.[5] Thus, it is likely that *Atoh1* gene expression is regulated by Notch signaling, leading to subsequent control of intestinal epithelial cell lineage decision of the crypt cells.

The regulation of Hath1, however, is less well understood in human intestine. In previous reports, regulation of *Atoh1* gene expression was assessed using the mouse or chicken promoter region,[11,12] but the critical domains of the mouse and chicken sequences are not completely conserved in the Hath1 promoter region and enhancer region. To date, the regulation of *Hath1* gene expression has not been assessed using the human sequence. In particular, it remains unknown how *Hath1* gene expression is suppressed by Notch signaling in the intestine. It also remains unknown whether goblet cell depletion in UC is affected by Hath1 expression in intestinal epithelial cells.

In this study we demonstrated that Hes1 expression via Notch signaling is enough to suppress the *Hath1* gene by directly binding to the 5′ promoter region of Hath1. In UC, the cooperation of Hes1 and caudal type homeobox 2 (CDX2) caused the suppression of Hath1, resulting in the goblet cell depletion.

MATERIALS AND METHODS

Cell Culture

Human colon carcinoma-derived LS174T cells were maintained in minimum essential medium supplemented with 10% fetal bovine serum and 1% penicillin-streptomycin, 4 mM L-glutamine. Except where indicated otherwise, cells were seeded at a density of 5×10^5 cells/mL in each experiment. Cell cultures and transfections of plasmid DNA were performed as previously described.[6] A cell line expressing Notch1 intracellular domain (NICD), Hes1, HeyL (Tet-On NICD, Tet-On Hes1, Tet-On HeyL cells) under the control of doxycycline (DOX, 100 ng/mL, ClonTech, Palo Alto, CA) was generated as previously described.[8] The cell lines were supplemented with Blastcidin (7.5 μg/mL, Invitrogen, La Jolla, CA) and Zeocin (750 μg/mL, Invitrogen) for maintenance. The inhibition of Notch signaling was achieved by the addition of LY411,575 (1 μM).

Quantitative Real-time Polymerase Chain Reaction (PCR)

Total RNA was isolated with Trizol reagent (Invitrogen) according to the manufacturer's instructions. Aliquots of 1 μg of total RNA were used for cDNA synthesis in 20 μL of reaction volume. One microliter of cDNA was amplified with Cyber Green in a 20-μL reaction as previously described.[6] The primer sequences in this study are summarized in Supporting Information Table S1.

Plasmids

5′ Hath1 reporter plasmid was generated by cloning a 1031-bp sequence 5′ of the human *Hath1* gene (corresponding to −1,029 to +2 of the promoter region) into a pGL4 basic vector (Promega, Madison, WI). Hath1 reporter plasmid containing the 3′ region was generated by cloning a 4811-bp sequence 3′ of the human *Hath1* gene (corresponding to +1401 to +6211 of the Hath1 genome) into the 5′ Hath1 reporter plasmid. Internal deletion mutants of the 5′ Hath1 reporter plasmid in which three Hes1 binding sites CACGCG (−305 to −300, −269 to −264, −159 to −154) were replaced with GTCGAC were constructed by PCR-mediated mutagenesis.[13] Doxycycline-dependent expression of NICD was achieved by cloning the gene encoding the intracellular portion of the mouse Notch1 into the pcDNA4/TO/myc-his vector (Invitrogen).[8] Doxycycline-dependent expression of Hes1 was achieved by cloning the gene encoding rat Hes1 into the pcDNA4/TO/myc-his vector (Invitrogen). Doxycycline-dependent expression of HeyL was achieved by cloning the gene encoding human HeyL into the pcDNA4/TO/myc-his vector (Invitrogen). All constructs were confirmed by DNA sequencing.

Luciferase Assays

LS174T cell seeded in a 6-well plate culture dish were transfected with 4 μg of reporter plasmid along with 10 ng of pRL-tk plasmid (Promega). Cells were harvested 36 hours after transfection, lysed by three cycles of freezing and thawing, and the luciferase activities in each sample as indicated by arbitrary unit were normalized against Renilla luciferase activities as previously described.[10]

Chromatin Immunoprecipitation Assay

A chromatin immunoprecipitation (ChIP) assay was performed essentially as previously described with some modifications.[6] LS174T/Hes1 cells were seeded onto a 150-mm dish, then stimulated with DOX or left untreated for 12 hours. Immunoprecipitation was performed overnight at 4°C with 10 μg of an anti-Hes1 (a kind gift from Dr. T. Sudo), normal mouse immunoglobulin G (sc-2025, Santa Cruz Biotechnology, Santa Cruz, CA), or an anti-histone H3 antibody (Abcam,

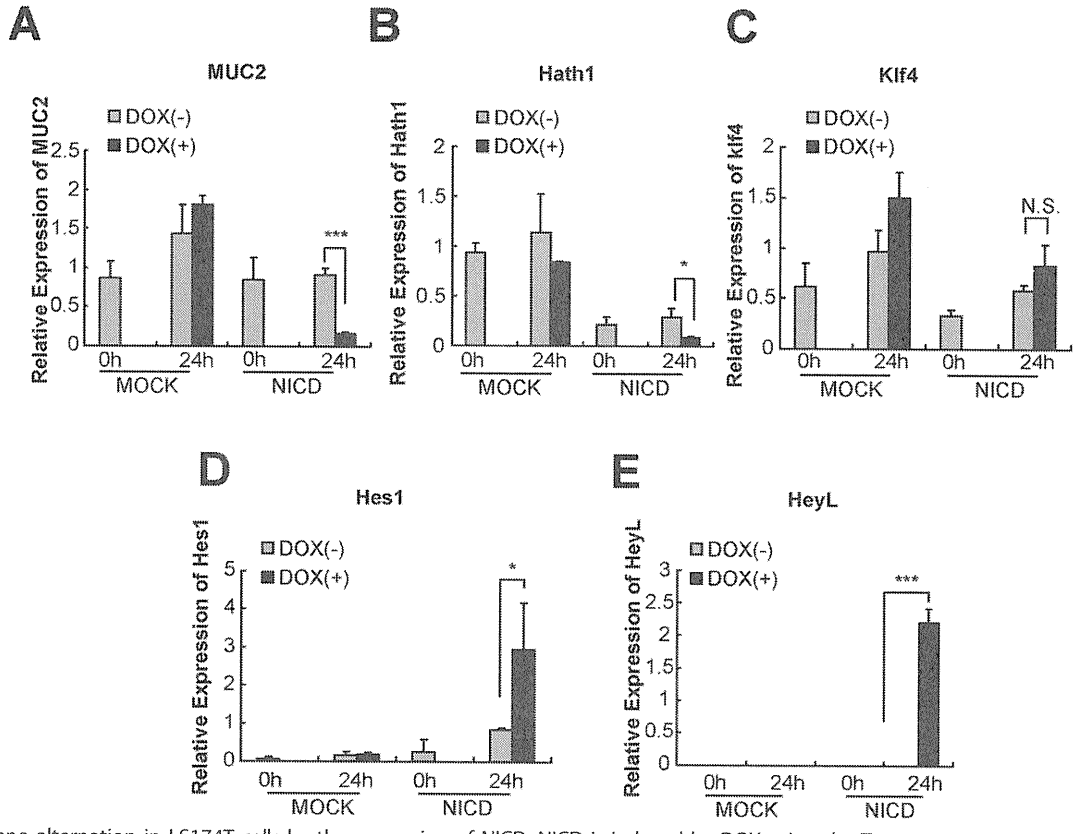

FIGURE 1. Gene alternation in LS174T cells by the expression of NICD. NICD is induced by DOX using the Tet-on system to mimic the acceleration of the Notch signal in LS174T cells. NICD expression by DOX decreased the expression of MUC2 (A) and Hath1 (B) genes. Klf4 gene expression was not affected (C). NICD also induced expression of Hes family genes such as Hes1 (D) and HeyL (E). ($^{*}P < 0.05$, $^{***}P < 0.001$, $n = 3$).

Cambridge, MA). The genomic DNA fragments in the immunoprecipitated samples were analyzed by PCR using primers indicating the positions on the genomic DNA relative to the translation start site (Supporting Information Table 1). The same amounts of DNA samples were analyzed by conventional PCR in parallel with the following parameters: denaturation at 94°C for 15 seconds, annealing at 60°C for 30 seconds, and extension at 68°C for 60 seconds for 45 cycles. The products were resolved by agarose gel electrophoresis, stained with ethidium bromide, and visualized using an ImageQuant TL system (GE Healthcare, Milwaukee, WI).[6] The primer sequences in this study are summarized in Supporting Information Table S1.

Human Intestinal Tissue Specimens

Human tissue specimens were obtained from patients who underwent endoscopic examination or surgery at Yokohama Municipal General Hospital or Tokyo Medical and Dental University Hospital. Normal colonic mucosa was obtained from patients with colorectal cancer who underwent colectomy. Each of three patients with UC and colon cancer were examined. Written informed consent was obtained from each patient and the study was approved by the Ethics Committee of both Yokohama Municipal General Hospital and Tokyo Medical and Dental University.

Immunohistochemistry

Hath1 antibody (1:5000) was originally generated as previously described. Hes1 antibody (1:10,000) was the same as in the ChIP assay. Fresh frozen tissue was used after microwave treatment (500W, 10 minutes) in 10 mM citrate buffer for Hath1 and Hes1. The standard ABC method (Vectastain; Vector Laboratories, Burlingame, CA) was used, and staining was developed by addition of diaminobenzidine (Vector Laboratories).

Statistical Analyses

Quantitative real-time PCR analyses were statistically analyzed with Student's *t*-test. *P* less than 0.05 was considered statistically significant.

RESULTS

Notch Signaling Suppresses *Hath1* Gene Expression But Not Kuppel-like Factor 4 (Klf4) Gene in Human IECs

Expression of Atoh1 seems to be regulated at its transcriptional level, as forced expression of NICD in murine IECs causes the decrease of Atoh1 mRNA expression and subsequent depletion of goblet cells in vivo.[5] We therefore assessed the effect of the Notch signal on the expression of

Hath1 in a human intestinal epithelial cell line, LS174T cells. NICD is induced by DOX using a Tet-on system to mimic the acceleration of the Notch signal. NICD expression showed not only the decrease of Mucin2 (MUC2) expression but also a significant decrease of *Hath1* gene expression (Fig. 1A,B). We also assessed Klf4 gene expression by NICD expression because Klf4 is also essential to goblet cell differentiation.[14] Klf4 gene expression, however, was not affected by forced NICD expression (Fig. 1C), since it is suggested that the suppression of goblet cell phenotypic gene expression by Notch signaling is independent of Klf4 expression.

To assess how Notch signaling suppresses the gene expression of Hath1, we selected the Hes1 and HeyL genes as possible suppressors, based on previous identification of the Hes family genes induced by NICD in LS174T cells using a microarray system.[8] We confirmed that the gene expression of Hes1 and HeyL was markedly induced by NICD expression (Fig. 1D,E).

Hes1 But Not HeyL Suppresses *Hath1* Gene Expression in Human IECs, Resulting in the Decrease of MUC2 Gene Expression

To assess which genes suppress the *Hath1* gene expression, we generated cells (LS174T Tet-on Hes1 cells and LS174T Tet-on HeyL cells) in which either Hes1 or HeyL is induced by DOX using the Tet-on system, respectively. Forced expression of Hes1 alone showed a significant decrease of MUC2 gene expression following the decrease of *Hath1* gene expression (Fig. 2A,B). In contrast, HeyL induction alone did not change the expression of either MUC2 (Fig. 2A) or Hath1 genes (Fig. 2B). Moreover, neither Hes1 nor HeyL induction affected Klf4 gene expression (Fig. 2C). These results are compatible with previous reports that the depletion of Hes1 in a mouse model upregulated Atoh1 mRNA expression in intestinal epithelial cells, resulting in the hyperplasia of the goblet cells.[15] Conversely, the finding that Klf4 was not affected by the Notch signaling differs from previous reports.[16]

Hes1 Expression Alone Is a Sufficient Condition for the Repression of the Phenotypic Gene Expression of Goblet Cells by Notch Signaling

To further analyze the functional role of Notch signaling in the differentiation of IECs, we next asked whether Hes1 expression alone is enough to compensate for the suppression of *Hath1* gene expression in Notch signaling. To inhibit the Notch signaling, LS174T Tet-on Hes1 cells were treated with gamma-secretase inhibitor (GSI), which prevents the separation of NICD from the Notch receptor. Notch signal inhibition by GSI treatment alone showed a significant decrease of Hes1 gene expression (Fig. 3A), in contrast to marked induction of MUC2

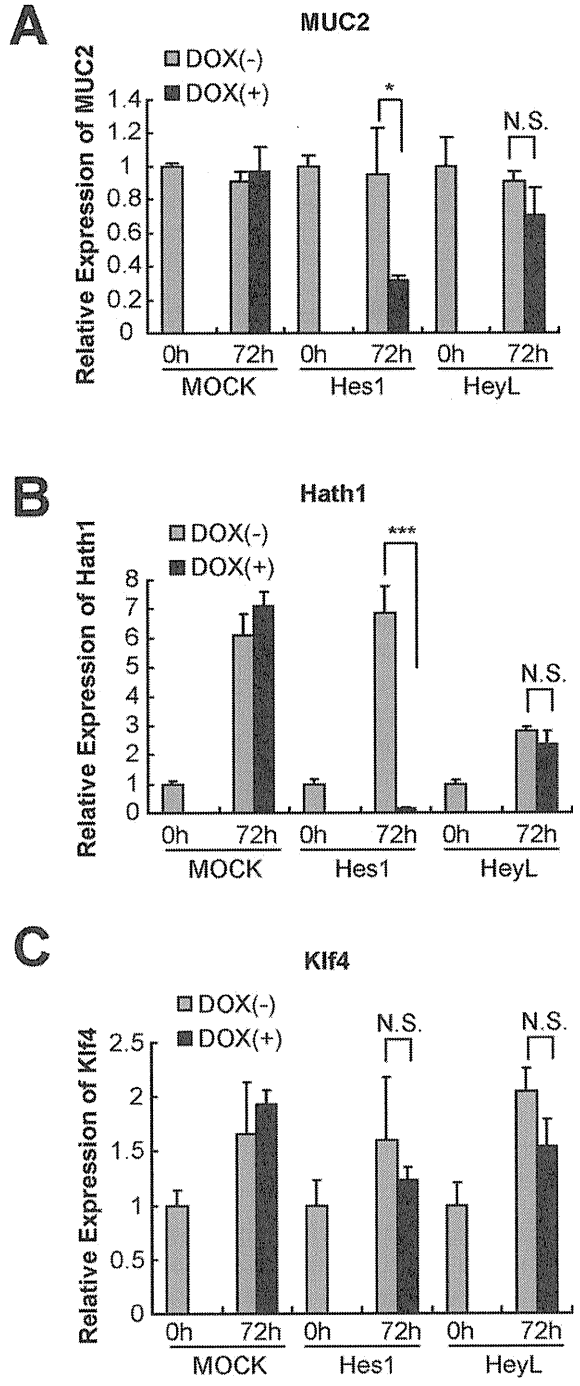

FIGURE 2. Gene alternation in LS174T cells by the expression of either Hes1 or HeyL. (A) Hes1 or HeyL was induced by DOX in LS174T Tet-on Hes1 cells or LS174T Tet-on HeyL cells, respectively. Hes1 induction significantly decreased MUC2 gene expression. (B) Hes1 induction resulted in a significant decrease of Hath1. (C) Neither Hes1 nor HeyL induction affected Klf4 gene expression. (*$P < 0.05$, ***$P < 0.001$, $n = 3$).

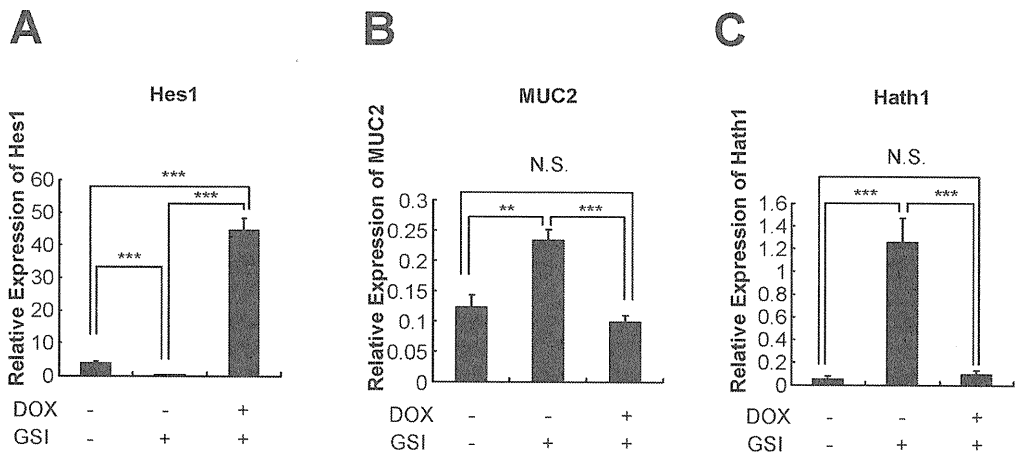

FIGURE 3. Hes1 expression is enough to suppress intestinal cell differentiation by Notch signaling. (A) LS174T Tet-on Hes1 cells were treated with GSI, which prevents the separation of NICD from the Notch receptor. GSI treatment alone significantly decreased Hes1 gene expression. Hes1 was induced by DOX in addition to GSI. (B) GSI markedly induced MUC2 gene expression. Hes1 induction by DOX in GSI-treated cells restored MUC2 gene expression to the level in untreated cells. (C) GSI markedly induced *Hath1* gene expression. Hes1 induction by DOX in GSI-treated cells restored *Hath1* gene expression to the level in untreated cells. (**$P < 0.01$, ***$P < 0.001$, $n = 3$).

gene expression (Fig. 3B) following the induction of the *Hath1* gene (Fig. 3C). Interestingly, the Hes1 gene was expressed by DOX when Notch signaling was inhibited by GSI (Fig. 3A), while Hath1 expression was restored to the level in untreated cells (Fig. 3C). Moreover, MUC2 gene expression was also decreased by Hes1 expression alone (Fig. 3B).

These results indicate that Hes1 might be a mainstream of Notch signaling to suppress the phenotypic gene expression of goblet cells in human intestine.

Previous results raised the question of whether Hath1 is essential for expression of the MUC2 gene by Notch signaling inhibition. To assess the importance of the *Hath1* gene for MUC2 expression, the effect of silencing the *Hath1* gene using siRNA system was examined in LS174T cells in the Notch signaling-inhibited state. *Hath1* gene silencing resulted in cancellation of the *Hath1* gene expression induced by GSI treatment and restoration of MUC2 expression to the level in untreated cells (Supporting Information Fig. 1).

These results together suggest that Notch signaling affects the gene expression of Hath1 but not Klf4 to decide the fate of IECs.

HES1 Suppresses the Transcriptional Activity of Hath1 Via the 5′ Promoter Region

It has been reported that expression of Math1, the mouse homolog of Atoh1, was suppressed by ZIC1 or HIC1 via its 3′ region.[12,17] However, it has never been shown how Hes1 suppresses the transcriptional activity of Hath1 via Notch signaling. To assess the regulation of Hath1 transcriptional activity, we constructed a reporter plasmid containing the 1000-bp upstream 5′ region of Hath1. Hath1 reporter plasmid was transfected into LS174T Tet-on Hes1 cells or LS174T cells transfected with a mock plasmid. Hes1 induction by DOX showed a significant decrease of the transcriptional activity on Hath1, whereas the mock plasmid did not change its transcriptional activity (Fig. 4A). We then found three regions that matched the consensus sequence for binding Hes1, the Class C site,[18] in the 1000-bp upstream region of Hath1. We therefore constructed a reporter plasmid in which all regions of the Hes1 binding site in the 1000-bp upstream region of Hath1 were deleted. As expected, reporter activity of the deletion mutant construct was not suppressed by Hes1 expression. We next constructed mutants in which one of the binding sites of Hes1 in the 1000-bp upstream region of Hath1 was deleted. Interestingly, only the mutant construct lacking the second region of the Hes1 binding site was not affected by Hes1, indicating that Hes1 might directly suppress the Hath1 transcriptional activity to bind to the second region of the Hes1 binding site (Fig. 4A).

In chicken and mouse models, Atoh1 expression is regulated only by the 3′ region of Atoh1 that contains both the enhancer region and the repressor region.[12,19] We also found a homologous sequence of the enhancer region in the 3′ region of Hath1, and a Hes1 binding site in this enhancer region of Hath1. We therefore constructed a Hath1 reporter plasmid containing the 3′ region of Hath1 behind the luciferase sequence. As before, Hes1 suppressed Hath1 transcriptional activity. Moreover, deletion mutants of the Hes1 binding site in the 5′ region of Hath1 were also unaffected by Hes1 expression, indicating that the Hes1 binding site of the 3′ region might not affect Hath1 suppression by Hes1 (Fig. 4B).

HES1 Binds Directly to the 5′ Promoter Region of Hath1

To confirm the binding of Hes1 to Hath1 promoter region, we performed a ChIP assay. The region immunoprecipitated by Hes1 antibody was amplified only in the 5′ region